How to Process LADCP Data For Vertical Velocity (w) and Derive Parameterized Estimates for Turbulent Kinetic Energy Dissipation (ϵ) using `LADCP_w` Software V2.2

A.M. Thurnherr
`athurnherr@mailbox.org`

December 6, 2022

Synopsis. This manual is intended as a "cookbook," describing how to derive profiles of vertical ocean velocity, vertical kinetic energy (VKE) and VKE-derived estimates of turbulent dissipation from data collected with standard LADCP/CTD systems. No special LADCP setup is required for vertical-velocity processing. As a result, vertical velocity, VKE and turbulent dissipation can be derived from many of the archived LADCP data sets. The `LADCP_w` software described in this manual is freely available for download from `http://www.ldeo.columbia.edu/LADCP`.

Contents

1 Introduction

1.1 Preliminary Comments

This manual is intended as a "cookbook," describing how to derive profiles of vertical ocean velocity (w_{ocean}, Sections 2–4), Vertical Kinetic Energy (VKE) and VKE-derived dissipation (ϵ_{VKE}, Section 5) from data collected with standard LADCP/CTD systems, using processing software available at `http://www.ldeo.columbia.edu/LADCP`. *No special LADCP setup is required for vertical-velocity processing. In particular, vertical velocities can be calculated from archived LADCP data, as long as pressure time series of adequate temporal resolution and quality are available*[1]. The software is a fairly complex implementation of a simple method that consists in subtracting vertical package velocity (w_{CTD}), derived from CTD pressure time series, from the ADCP-derived vertical velocity measurements (w_{ADCP}), before binning the resulting ocean velocities ($w_{\mathrm{ocean}} = w_{\mathrm{ADCP}} - w_{\mathrm{CTD}}$) in depth *(Thurnherr,* 2011). The processing software is implemented in the `perl` programming language and has been tested on UN*X systems, including MacOSX, FreeBSD and Linux. All source files use tab stops every 4 columns; for correct formatting use, e.g. `less -x4` or an editor where the tab separation can be changed.

This document describes version 1.5 of the `LADCP_w` software. Older versions have significant bugs and should no longer be used. Each output file from this software contains the version of the processing-software in the header (meta-data). The diagnostic plots are also labeled with the processing version.

1.2 Comparison with Horizontal Velocity Processing

Processing LADCP data for vertical velocity is conceptually much simpler than horizontal-velocity processing, which requires simultaneous estimation of both ocean and CTD package velocity *(Firing and Gordon,* 1990; *Fischer and Visbeck,* 1993a; *Visbeck,* 2002). While the unknown horizontal CTD-package velocity required to obtain ocean velocity from the relative measurements must be inferred from external constraints in case of horizontal velocity, the vertical package velocity w_{CTD} is known at all times. This has several important consequences:

1. Random measurement errors in the vertical velocities at a given depth derived from a downward pointing ADCP ("downlooker") and from an "uplooker" are independent, as they do not use any common data. (The two instrument sample the velocity at a given depth at different times.) Differences between uplooker and downlooker-derived w_{ocean} data therefore provide a quantitative metric of measurement uncertainty due to random errors (but not bias).

2. Profiles with gaps, e.g. due to insufficient acoustic scattering at depth, can be processed without any particular difficulties.

3. Because of the random-walk error accumulation, instrument range is the most important parameter affecting the quality of horizontal LADCP velocities *(Firing and Gordon,* 1990; *Visbeck,* 2002; *Thurnherr,* 2010). For vertical velocities, random error (but not bias) can be reduced by decreasing the vertical resolution of the binned profiles during post-processing. This allows calculation of w_{ocean} in some regions where the acoustic backscatter is too weak (instrument range too short) for horizontal-velocity processing.

---

[1]In practice this means minimally processed 24 Hz time series from SBE 911plus CTD systems.

There are additional important differences between processing LADCP data for horizontal and vertical velocities:

1. Horizontal ocean velocities are mostly dominated by processes with timescales that are long compared to typical LADCP/CTD cast durations. As a result, down- and upcast data are usually combined to yield cast-time averaged profiles. In contrast, vertical velocities are mostly dominated by internal waves near the buoyancy frequency (e.g. *Thurnherr et al.*, 2014), i.e. with time scales that are not long compared to typical CTD/LADCP sampling time scales. As a result, down- and upcast w_ocean data must be processed separately, yielding two profiles from each cast.

2. Good heading (compass) data are required for horizontal-velocity LADCP processing. LADCP data collected near the magnetic poles, in particular, cannot be processed for horizontal velocity. In contrast, heading data are not used at all for w_ocean LADCP processing, i.e. data from the magnetic poles or from instruments with bad compasses can be processed for vertical velocity.

It is important to emphasize that *vertical velocity can be measured with LADCP systems in many regions where horizontal velocity measurements are impossible, including where backscatter is low, such as the centers of sub-tropical gyres, and in high-latitude regions close to the magnetic poles.*

1.3   Software Requirements and Installation

The processing software for vertical LADCP velocities is implemented in the `perl` programming language, which is pre-installed on all UN*X systems. Diagnostic plots are produced with the `Generic Mapping Tools` (GMT), a set of UN*X tools to produce Postscript plots from ASCII input files. The following software is required to process LADCP/CTD data for vertical velocity:

Generic Mapping Tools (GMT) GMT must be installed and the GMT binary directory must be included in the search path of the shell[2]. GMT version 6 is required.

ANTSlib This undocumented library, available at `www.ldeo.columbia.edu/LADCP`, provides a general data processing and I/O framework. The installation directory must be added to the shell's search path.

ADCP_tools This partially documented tool kit provides additional required libraries, as well as a number of ADCP utilities, e.g. for splitting ADCP files from tow-yos and yo-yos into individual casts. The ADCP Tools are available at `www.ldeo.columbia.edu/LADCP`. The installation directory must be added to the shell's search path.

LADCP_w The vertical-velocity processing software is implemented as several separate command-line utilities (described below). It is available at `www.ldeo.columbia.edu/LADCP`. The installation directory must be added to the shell's search path.

Once all required software has been installed, the installation can be tested by running

```
LADCP_w_ocean -V
```

from any directory. If any of the prerequisites are missing or if the shell search path is not set correctly the program aborts with an error message. If the installation is complete, on the other hand, a short version and copyright message is produced instead. Running `LADCP_w_ocean` or any other of the utilities described below without command-line arguments produces a usage message with a brief description of the command-line options and arguments.

---

[2]Familiarity with basic UN*X shell concepts is assumed in this manual.

1.4 Processing Overview

Vertical-velocity processing is carried out in several consecutive steps, which are implemented as separate command-line utilities to allow selective re-processing:

1. *Calculate vertical package velocity* w_{CTD} *with the* **LADCP_w_CTD** *utility.* Input: 24 Hz CTD time series. Output: 6 Hz time series of pre-processed CTD data, including low-pass w_{CTD}, as well as diagnostic plots. For details, see Section 2 below.

2. *Calculate vertical ocean velocity* w_{ocean} *with the* **LADCP_w_ocean** *utility.* Input: 1) 6 Hz time series of pre-processed CTD data; 2) ADCP data file; 4) Processing control file. Output: Processed vertical ocean velocities, as well as diagnostic data and plots. For details, see Section 3 below.

3. *Optionally post-process* w_{ocean} *with the* **LADCP_w_postproc** *utility.* Common post-processing steps include bias correction and manual data editing to remove bad measurements. Primarily for quality control, uplooker and downlooker data from dual-headed LADCP systems can be combined. Input: One or two **LADCP_w_ocean** output files, and a file with data-editing instructions. Output: Edited w_{ocean} profile. For details, see Section 4.3 below.

4. *Estimate finestructure Vertical Kinetic Energy density (VKE) and parameterized kinetic energy dissipation* ϵ_{VKE} *with the* **LADCP_VKE** *utility.* This utility implements a finestructure parameterization for dissipation of turbulent kinetic energy *(Thurnherr et al., 2015)*. Input: Vertical velocity profile from **LADCP_w_ocean** or **LADCP_w_postproc**. Output: Profiles of VKE and parameterized dissipation, as well as diagnostic data and plots. For details, see Section 5.

For processing, every profile must be assigned a unique *profile id* (usually numerical), which is used to construct file names and to select profile-specific processing parameters. Often it makes sense to use the CTD station number as the *profile id.* In addition to the *profile id,* every processed profile is additionally associated with a *run label*, which can be any character string. This allows multiple processing runs for a single profile, which is used, for example, to process downlooker and uplooker files from dual-headed LADCP systems.

1.5 Input/Output Data

ADCP Input Data. Binary data in the Teledyne/RDI PD0 format are accepted as input. Supported TRDI instrument types include NB150, BB150, WH150, WH300, WH600, WH1200, and the Explorer DVL. Supported Nortek instruments include the SIG100, with the PD0 file created with the Nortek file conversion utility.

CTD Input Data. Either binary or ASCII 24 Hz `.cnv` time-series files from SBE 911plus systems are accepted as input. Alternatively, the CTD data can be supplied in a simple ASCII CSV format (Appendix A). In case of SBE `.cnv` files, the header must include the latitude of the station, and the file must contain pressure (`prDM`), *in situ* temperature (`t090c` and/or `t190c`) and conductivity (`c0S/m` or `c0mS/cm` and/or `c1S/m` or `c1mS/cm`) fields. If the CTD file contains a header field called `station`, the content of this field is taken as the default *profile id.*

In case of transmission errors, SBE 911plus CTD systems drop scans without accounting for the dropped scans in the time fields. As a result, dropped scans appear as CTD clock jumps, which require special treatment during vertical velocity processing (Appendix B.1). For CTD `.cnv` files that also contain the `timeY` and `modError` fields, dropped scans are handled automatically, which is much more accurate than manual handling.

Output Data. All output files use a whitespace-delimited ASCII file format called the ANTS format. The "#" character is used for comments and metadata header lines; the string `nan` is used to indicate missing values. ANTS files can easily be read by many software packages, possibly after manually removing the headers. The file layout (association of field names with data columns) is defined by the last header line beginning with `#ANTS#FIELDS#`. Header lines beginning with `#ANTS#PARAMS#` define meta-data parameters. The `Matlab` script `loadANTS.m`, which resides in the installation directory of the `LADCP_w` software, can be used to load ANTS files, including metadata, into Matlab. A Python interface is overdue.

Diagnostic plots. All plots produced by the processing software are in Postscript (`.ps`) format with loose bounding boxes (standard GMT6 output).
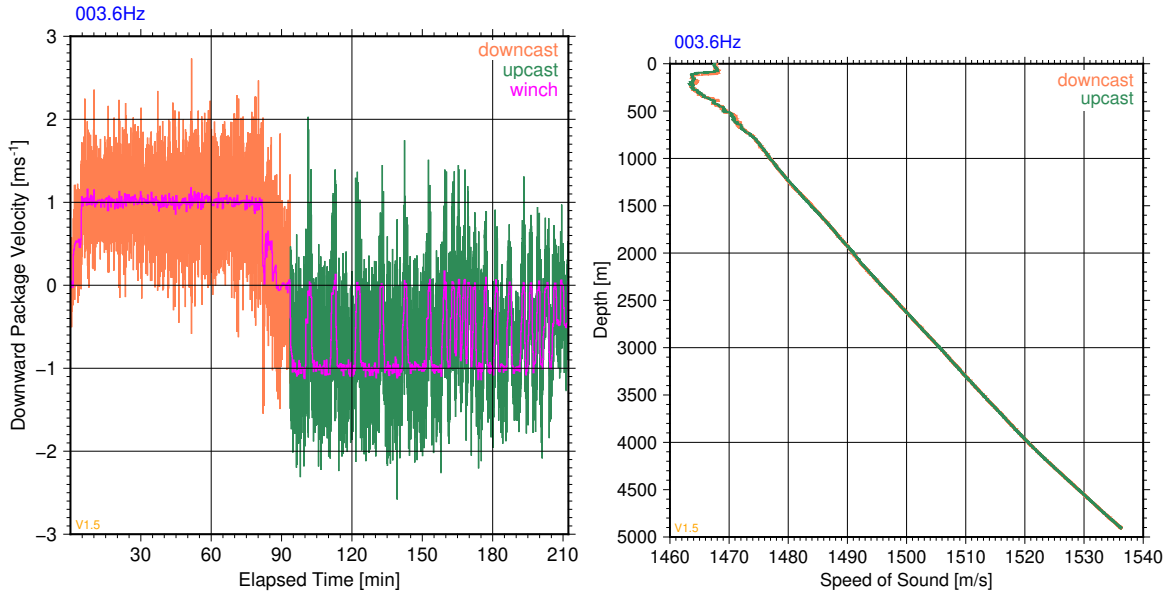
Figure 1: Example plots of output of LADCP_w_CTD from DIMES US2 station 003 in the Southern Ocean. Left panel: Time series of vertical package velocity. Right panel: Sound speed profile.

2 Calculating Vertical Package Velocity (LADCP_w_CTD)

In a first processing step, 24 Hz CTD time-series data are pre-processed with the LADCP_w_CTD utility to derive cleaned 6 Hz time series of depth, sound speed, vertical package velocity, and temperature. The vertical package velocity is low-pass filtered to remove measurement noise; based on tests carried out with an early version of the processing software, a default low-frequency cut-off of 2 s is used.[3] Additionally, the minimum observed pressure is subtracted from all pressure measurements to ensure non-negativity.

LADCP_w_CTD takes the name of the CTD file as an argument and, often[4] also a profile id supplied with the -i command-line option. If there are no latitude/longitude information in the header, the station location must be specified with the -l option. The preferred input formats of CTD files are SBE .cnv binary or ASCII files (HEX .cnv files are not supported). [If .cnv files are not available the CTD time series data can also be supplied in a simple ASCII CSV format (Appendix A).] The CTD data files must include pressure (prdM or prDM), temperature (t090C or tv290C) and conductivity (c0S/m or c0mS/cm). Transmission glitches cause scans to be dropped from CTD files collected with SBE 911plus systems. Dropped CTD scans require special treatment during processing (Appendix B.1). CTD .cnv input files containing the timeY[5] and modError fields are automatically corrected for dropped scans, obviating the need for manual intervention. If the .cnv contains GPS data (lat and lon), those are pre-processed and stored in the output time series, in order to make the files produced by LADCP_w_CTD -s 1 useful for horizontal-velocity processing.

By default, LADCP_w_CTD only displays error messages. In order to see progress, use -v 1; for

---

[3]The low-pass cutoff can be modified with a command-line option to LADCP_w_CTD.

[4]For CTD .cnv files with the correct profile id in the station header field, -i is not required.

[5]The timeY field is only available for profiles recorded with the "Scan time added" option selected in the instrument configuration.

diagnostic output use `-v 2`. For example, the command

```
LADCP_w_CTD -i 8 -v 2 oc46802008.cnv
```

processes the data in the file `oc46802008.cnv` with diagnostic output on screen, and produces the following three output files:

008.6Hz Cleaned-up and low-pass filtered 6 Hz time-series of CTD measurements (pressure, temperature, conductivity), and derived quantities (depth, salinity, sound speed, vertical package velocity).

008_wpkg.ps Diagnostic plot of of vertical package velocity time series (e.g. Figure 1, left panel).

008_sspd.ps Diagnostic plot of sound speed profile (e.g. Figure 1, right panel).

The user must ensure that the CTD time series used for vertical-velocity processing are free from significant glitches that escaped the automatic cleanup. Therefore, all diagnostic plots produced by **LADCP_w_CTD** should be inspected. [Figure 1 shows examples from a station in the Southern Ocean for reference. Note that the maximum downward package velocity during the downcast is nearly $3\,\text{m}\cdot\text{s}^{-1}$, i.e. almost $3\times$ the winch speed.] Pressure spikes, in particular, introduce package-velocity anomalies that typically cause the time-lagging algorithm used to merge the CTD with the ADCP data (Section 3) to fail. Other errors in the CTD data often do not cause processing to fail, but they increase the vertical-velocity errors and the erroneous data should, therefore, be removed. Profiles for which the automatic data editing implemented in **LADCP_w_CTD** is insufficient must be pre-cleaned by replacing bad values in the input file with **nan** strings. *No scans must be removed from or added to the CNV files that serve as input to LADCP_w_CTD.*

3 Calculating Vertical Ocean Velocity (`LADCP_w_ocean`)

3.1 Synopsis

In a second processing step the `LADCP_w_ocean` utility is used to calculate w_{ocean} from combined LADCP and CTD data. As input, `LADCP_w_ocean` requires a pre-processed CTD time series (Section 2) as well as a binary ADCP file. (The up- and downlooker data from dual-head LADCP systems are processed separately, but the data can easily be combined during post-processing; Section 4.3.) `LADCP_w_ocean` requires one or two command-line arguments:

`profile-id` This argument is mandatory and usually numeric. It is used to select the CTD and ADCP input files, set profile-specific processing parameters, and to create output file names.

`run-label` This argument is optional and can be any string. It is used to distinguish different processing runs for the same profile. For example, for dual-head LADCP systems the run labels `DL` and `UL` can be used for processing downlooker and uplooker data, respectively. If no run label is specified the label `default` is assumed. Each run label has its own associated output subdirectory, using the label as its name. The output directory is automatically created if it does not already exist.

It is not possible to specify input or output files for `LADCP_w_ocean` on the command line. Rather, `profile-id` and `run-label` are used to define the input and output filenames in the processing-configuration file (Section 3.2), which is also used to set the many configurable parameters controlling different aspects of processing. Some of the of the most commonly modified processing parameters can also be set with command-line options, however, including the following:

Screen verbosity (`-v`). `LADCP_w_ocean` produces log output both on screen and in a log file. The `-v` option is used to set the verbosity level (0–3) for the screen output only, with `-v 0` producing only error messages, `-v 1` also including warnings, `-v 2` producing a substantial amount of diagnostic output, and `-v 3` listing everything, including debugging messages. Default screen verbosity level is 1, and the log files always contain level 2 output.

Time lagging (`-i`, `-n`, `-w`). Determining the temporal alignment between the CTD and LADCP data is crucially important for obtaining good vertical ocean velocities. The time-lagging algorithm involves three steps: i) An initial estimate is made based on the time when each profile reaches 10% of its maximum depth; this algorithm can be overridden by using the `-i` option. ii) A coarse-resolution time lag is calculated from 1 Hz CTD data. iii) A fine-resolution time lag is calculated using the full-resolution (6 Hz) CTD data. For steps ii and iii, the data are split into windows, controlled with the `-n` and `-w` options.

Water depth (`-h`). Knowledge of the water depth is important for editing measurements affected by previous-ping interference (PPI) and sidelobe contamination from the seabed. While the water depth is usually detected correctly by downlooking ADCPs, it has to be supplied manually for processing uplooker[6] data. The easiest way to do this is to specify the water depth with the `-h` command-line option to `LADCP_w_ocean`. Either a numerical value (water depth in meters) or the name of the corresponding downlooker w_{ocean} profile, which contains the water depth as meta data, can be provided as an option argument.

---

[6]Even LADCP data from upward-looking instruments can be severely degraded by sidelobe contamination from the seabed!

Output resolution (-o). With this option the vertical resolution of the output w_{ocean} profile can be set. In contrast to horizontal LADCP velocities, w_{ocean} profiles in regions of weak acoustic backscatter can often be improved by decreasing the vertical output resolution. Conversely, the output resolution can sometimes be increased in regions of strong backscatter to increase the vertical resolution. The default vertical resolution of $40\,\mathrm{m}$ is appropriate for many data sets.

3.2   Processing Configuration File (`ProcessingParams`)

There are numerous parameters controlling processing. A complete list, including documentation, can be found in the files `defaults.pl, default_paths.pl` and `default_output.pl` in the installation directory. The default parameter values are suitable for data sets collected with $300\,\mathrm{kHz}$ Workhorse instruments (WH300) with $8\,\mathrm{m}$ bin size; for different bin sizes and/or instruments some of the parameters likely need to be changed. The file `defaults.pl` should never be modified, however. Rather, non-default processing-parameter values should be set in a processing configuration file. This configuration file is read *after* processing the command-line options, i.e. definitions in the configuration file take precedence over command-line options.[7] There are several possible filenames for the configuration file. Given the run label `DL`, the following filenames are tried in order: `ProcessingParams.DL, ProcessingParams.default, ProcessingParams`. The first file that is found, is used. When `LADCP_w_ocean` is executed without a run label, only the latter two names are tried.

   The processing configuration files are `perl` scripts. When they are executed, the current profile id and run label are stored in the variables `$PROF` and `$RUN`, respectively, allowing profile- and run-specific parameters to be selected with `if`-statements. While all processing parameters have suitable defaults, at the very least the LADCP and CTD input file names must be defined in the variables `$LADCP_file` and `$CTD_file`. The following example code assumes that the LADCP and CTD data for profile 13 can be found in the files `./LADCP/013DL000.000` and `./CTD/013.6Hz`, respectively:

```
$LADCP_file = sprintf("LADCP/%03dDL000.000",$PROF);
$CTD_file = sprintf("CTD/%03d.6Hz",$PROF);
```

If the CTD and/or LADCP input files use inconsistent numbering, a simple lookup table can be implemented, for example, as follows:

```
if (($PROF == 1) && ($RUN eq "DL")) {
    $LADCP_file = "LADCP/003DL000.000";
    $CTD_file   = "CTD/002.6Hz";
} elsif (($PROF == 2) && ($RUN eq "DL")) {
    $LADCP_file = "LADCP/002DL000.000";
    $CTD_file   = "CTD/003.6Hz";
} else {
    die("cannot determine input files for profile $PROF run $RUN");
}
```

noting that the perl operators `=` and `eq` check for numerical and lexical (string) equality, respectively. Of course, it is also possible to add profile-specific processing parameters to the same `if`-statement.

---

[7]The only exception to this rule is that any expression supplied with the `-x` command-line option is executed after the configuration file has been processed.

3.3 Processing Output

3.3.1 Velocity Residuals, Errors, Accuracy and Precision

Every velocity sample from an LADCP system is the sum of three different contributions *(Visbeck, 2002)*, i.e.

$$w_{\text{measured}} = w_{\text{ocean}} + w_{\text{CTD}} + w_{\text{residual}}, \tag{1}$$

where the residual vertical velocity w_{residual} contains all the measurement and model errors[8]. Ideally the residual velocity should be randomly distributed in time and space — as described below, non-random structure in the residual velocity is used as a quality indicator for the vertical velocities.

While the residual velocities are intended to account for all measurement and model errors the separation of the measurements into its different contributions cannot be done perfectly. The processed profiles of vertical ocean velocity $w_{\text{ocean}}(z)$ are therefore not error free. From deployments on fixed bottom mounts it is clear that vertical velocity measurements of $300\,\text{kHz}$ TRDI Workhorse AD-CPs are associated with *biases* of a few mm·s^{-1} even without instrument motion. Consistent with this observation, cruise-averaged vertical velocities from several recent GO-SHIP repeat-hydrography cruises have magnitudes between $4\,\text{mm·s}^{-1}$ and $8\,\text{mm·s}^{-1}$ (see also Section 4.1). In addition to these biases, there are also "random" errors with unknown magnitudes and covariance scales. The magnitude of these errors can be estimated from velocity profiles collected with dual-head instruments. Based on two recent GO-SHIP cruises, these random errors appear to be of similar magnitude to the biases.

While the *accuracy* of individual w_{ocean} estimates is therefore not much lower than $1\,\text{cm·s}^{-1}$ the *precision* can be considerably better. The two VKE spectra shown in Fig. 1a of *Thurnherr et al.* (2015), for example, both show noise levels in VKE density of $\approx 10^{-4}\,\text{m}^2\text{·s}^{-2}\text{·(rad/m)}^{-1}$, which correspond (considering the resolution bandwidth) to a precision of 1.5–$2\,\text{mm·s}^{-1}$.

3.3.2 Output Files

`LADCP_w_ocean` creates several output files, all in a subdirectory that uses the run label as its name. (If no run label is specified on the command line, the label `default` is used in the `ProcessingParams` file, but the output directory is called `profiles`.) If the output directory does not exist it is created. Assuming that the downlooker data from profile 13 have been processed successfully with the command

```
LADCP_w_ocean 13 DL
```

the following data files were created:

`DL/013.log` Processing log output at verbosity level 2.

`DL/013.wprof` Gridded vertical velocity profiles; most fields are prefixed with `dc_`, `uc_` or `BT_`, indicating downcast, upcast and bottom-track variables, respectively. Each depth bin is associated with a nominal depth (bin center; `depth`) and height-above-bottom (when water depth is known; `hab`). Additional variables: `_elapsed` – mean elapsed time of all samples in the bin; `_w` and `_w.mad` – median and mean-absolute deviation of w_{ocean}; `_nsamp` – number of samples; `_lr_bp_res.rms` – *rms* beam-pair (`_w12` and `_w34`) residuals in 5-bin-thick layers (200 m by default); (`_depth` – mean depth; `_w12` and `_w34` – median of 2-beam vertical velocities; `_w12` and `_w34` median of quasi-horizontal 2-beam velocities. [For coordinate transformations, see Appendix C.]

---

[8]The processing model assumes, for example, that all downcast samples at a given depth are are taken at the same location and that there is no oceanographic variability while the samples are collected.

`DL/013.wsamp` Individual vertical velocity measurements (one record per bin for each ensemble). For each sample, the following information is recorded: ADCP ensemble number (`ensemble`), ADCP bin number (`bin`), elapsed time in seconds (`elapsed`), depth of measurement (`depth`), CTD depth (`CTD_depth`), downcast flag (`downcast`), 3-/4-beam vertical ocean velocity (`w`), two separate 2-beam vertical velocities (`w12` and `w34`), two quasi-horizontal 2-beam velocity components (`v12` and `v34`), gridding residuals of the 3-/4- and 2-beam solutions (`residual`, `residual12`, `residual34`), vertical package velocity (`CTD_w`), acceleration (`CTD_w_t`) and its time derivative (`CTD_w_tt`), measured vertical velocity (`LADCP_w`), reference-layer vertical velocity (`LADCP_reflr_w`), estimate of the winch velocity (`winch_w`), error velocity (`errvel`), correlation (`correlation`), echo amplitude (`echo_amplitude`), volume scattering coefficient (`Sv`) calculated with the method of *Deines* (1999) with an additional empirical correction for remaining bin-dependent biases, package attitude (`pitch`[9], `roll`, `tilt` and `heading`), 3-beam flag (`3_beam`), and sound speed (`svel`).

`DL/013.tis` Time series of ADCP records (one record per ensemble) with merged CTD information: ensemble number (`ensemble`), elapsed time in seconds (`elapsed`), downcast flag (`downcast`), CTD depth (`depth`), sound speed at the transducer (`xducer_sound_speed`), package attitude (`pitch`, `gimbal_pitch`, `roll`, `tilt` and `heading`), vertical package velocity (`CTD_w`), time derivative of vertical package acceleration (`CTD_w_tt`), mean and standard deviation of LADCP reference-layer vertical velocity (`LADCP_reflr_w` and `LADCP_reflr_w.sig`, respectively), and reference-layer ocean w (`reflr_ocean_w`).

In addition to those data files, a set of diagnostic plots are created. Figs. 2–5 show representative examples from high-quality profiles with both weak (left panels) and strong (right panels) vertical-velocity signals.

`DL/013_wprof.ps` This is the main diagnostic figure, showing downcast-, upcast- and bottom-tracked vertical velocity profiles, gridding statistics, profile summary information, as well as data-quality indicators (Figure 2). For data recorded in beam coordinates, the two 2-beam vertical velocities from both the up- and downcast are plotted separately with dashed and dotted lines, respectively. For data recorded in Earth coordinates, only a single solution is shown (e.g. upper right panel of Figure 10 in Appendix B). The information in these summary plots provides information on data quality:

Down- vs. upcast data. In contrast to the temporal variability associated with horizontal ocean velocity, which is associated with timescales that are long compared to the typical sampling time of a LADCP/CTD profile, vertical velocity variability is dominated by near-N "buoyancy waves." Since the typical buoyancy period varies from a few minutes in the strongly stratified upper ocean to a few hours in the weakly stratified abyss, down- and upcast w profiles cannot be expected to be similar, except near the bottom turning point. However, the statistics of w variability, especially the length scales and amplitudes, of the down- and upcast data should be similar. This is the case in the example profiles. Near the lower turning point of the profile the down- and upcast vertical velocities should be similar to each other. LADCP velocities near the surface and seabed are often contaminated by side-lobe interference, causing gaps in the processed profiles (red hashing in the figure).

Bottom Tracked Velocities. For downlooker profiles extending within range of the seabed, bottom-tracked vertical velocities are shown near the seabed (black). In the two examples, there is reasonable agreement between the bottom-track and the CTD-referenced profiles. Note that bottom-tracking is associated with its own errors.
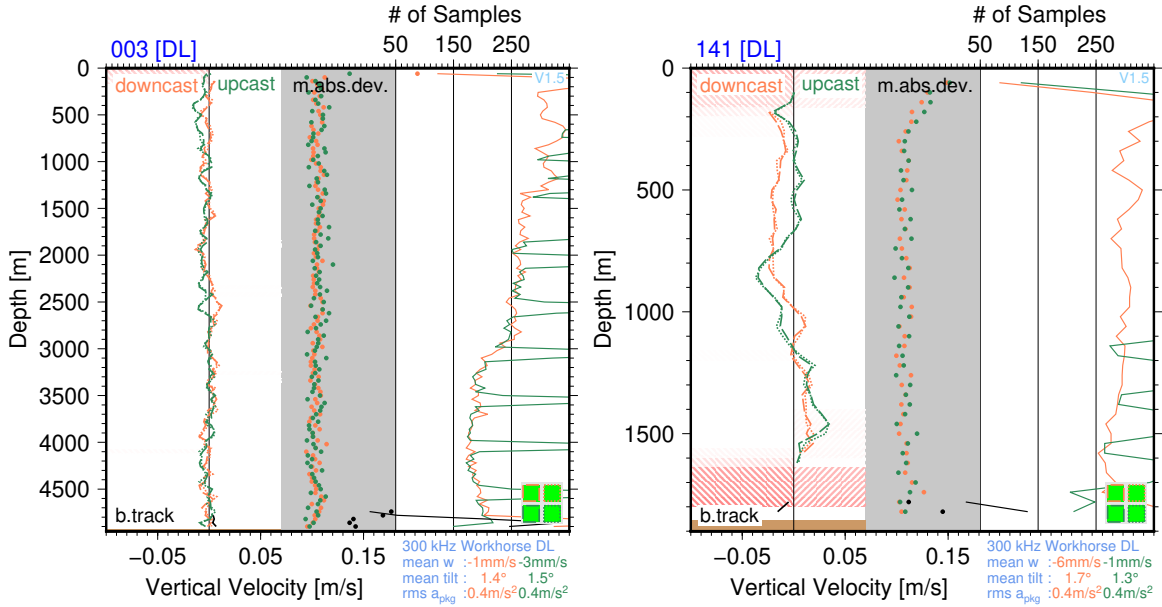
---

[9]Gimbal pitch, not TRDI pitch.

Figure 2: Example _wprof.ps diagnostic plots from two profiles from the DIMES US2 cruise with weak (left panel) and strong (right panel) vertical velocities; colors are used to distinguish between downcast (green), upcast (orange) and bottom-track (black) data. Blue labels above the figure panels show the profile-id and [run-label]. Summary information printed below the panels on the right includes instrument type and orientation, profile-averaged vertical velocity and instrument tilt, as well as *rms* vertical package acceleration (sea state). Each panel contains three different profile plots: i) 2-Beam vertical ocean velocity (median in each depth bin) plotted with dashed (w_{12}) and dotted (w_{34}) lines on the left and using the lower x-axis; bad data causes gaps in the profiles. ii) Corresponding mean-absolute-deviations (m.abs.dev.) plotted with bullets over gray background and also using the lower x-axis. iii) Corresponding number of samples plotted with solid lines on the right, using the upper x-axis. In addition to the summary information and profiles the panels also contain two quality indicators: i) four colored squares in the bottom-right figure corners, summarizing the main information from the DL/013_bin_residuals.ps diagnostic figure (e.g. Figure 3); ii) red hashing (downward trending for downcasts and upward-trending for upcasts) underlying the vertical-velocity profiles, summarizing the main information from the DL/013_residual_profs.ps diagnostic figure (e.g. Figure 4).

2-Beam Vertical Velocities. Some data problems, such as package-wake effects (Appendix B.3) and bad beams, cause disagreement between the two 2-beam solutions, which is easily visible in the _wprof.ps plots from profiles collected in beam coordinates.

Data Scatter. The middle profiles (green and orange bullets) show the data scatter in each depth bin in terms of mean absolute deviation from the median. The increase toward the surface apparent in the upper 200 m of both example profiles is quite typical for LADCP data.

Sampling. The right profiles in each figure panel show the number of samples in each depth bin. Bottle stops are clearly apparent during the upcasts (green). Bins with more than about 100 samples are typically well constrained; as the number of samples decreases the

13

quality of the vertical velocities decreases as well.

Instrument tilt. LADCP data are best when measured at small instrument-tilt angles, with indications that instrument tilt is related to vertical velocity biases. The mean tilt values printed in the figure panels can help detect problems with package attitude, such as kiting behavior during downcasts, which can seriously degrade the data quality. Note that there are no diagnostic plots showing instrument pitch, roll and heading behaviour produced during vertical velocity processing. Mean tilt angles below 2°, as in the case of the two example profiles, are excellent; mean tilt angles greater than about 5° are a potential concern, especially with regard to vertical velocity biases.

Sea state. The *rms* vertical package acceleration gives an indication of the heaving motion of the vessel, which co-varies with sea state. The heaving motion in the two example profiles is near the upper limit where LADCP work is typically possible. This illustrates that LADCP vertical velocities of excellent quality can be collected even with significant package motion.

Vertical-Velocity Residuals. [See Section 3.3.1 for a definition of velocity residuals.]

1. In the bottom right corner of each `_wprof` diagnostic figure there are four colored squares indicating the overall magnitudes of the vertical velocity residuals from the two beam pairs (left: beams 1-2, right: beams: 3-4) from the down- (upper row) and upcast (lower row). The squares summarize the information from another diagnostic figure (`_bin_residuals.ps`; see below), with green, yellow and red colors indicating good, suspect and likely bad data, respectively.

2. Diagonal red hashing underlying the w_{ocean} velocity profiles indicates layers of anomalously large velocity residuals, summarizing the information from yet another diagnostic figure (`_residual_profs.ps`; see below). Potential problems with the downcast data are indicated by downward-trending hash lines in the negative velocity half space; potential problems with the upcast data are indicated by upward-trending hash lines in the positive velocity half space; the more saturated the red the bigger the residuals. In both examples, there are large residuals in the upper 100 m or so, and in profile 141 (right figure panel) there are also large residuals in the bottom 300 m. Larger errors near the boundaries in LADCP profiles are likely related to sidelobe contamination.

Summary Information. Below the figure panels on the right there is a legend with profile summary information, including instrument type and orientation, mean vertical velocity and instrument tilt, as well as *rms* vertical package acceleration observed during the cast. For deep profiles (more than 2000 m or so), the mean vertical velocity provides an indication of bias errors; when the down- and up-cast biases differ by more than $5\,\mathrm{mm}\cdot\mathrm{s}^{-1}$ ($1\,\mathrm{cm}\cdot\mathrm{s}^{-1}$) the mean values are printed over yellow (red) background. Large package tilts degrade the LADCP data; this problem can sometimes be mitigated by adding ballast to the CTD package and/or by lowering the winch speed during downcasts. Vertical package acceleration is dominated by heave due to surface waves moving the ship, i.e. it varies with sea state. (Vertical package acceleration ranges from $\approx 0.02\,\mathrm{m}^2\cdot\mathrm{s}^{-1}$ for profiles taken in flat calm conditions to $>0.6\,\mathrm{m}^2\cdot\mathrm{s}^{-1}$ for profiles collected in heavy seas.) There is evidence that the quality of LADCP data is affected by sea state. Abnormally large package tilts and accelerations are marked with yellow (moderately large) and red (very large) background colors; blue background indicates very little surface-wave related package motion (e.g. in profiles collected in sea ice), which can cause problems with time lagging.
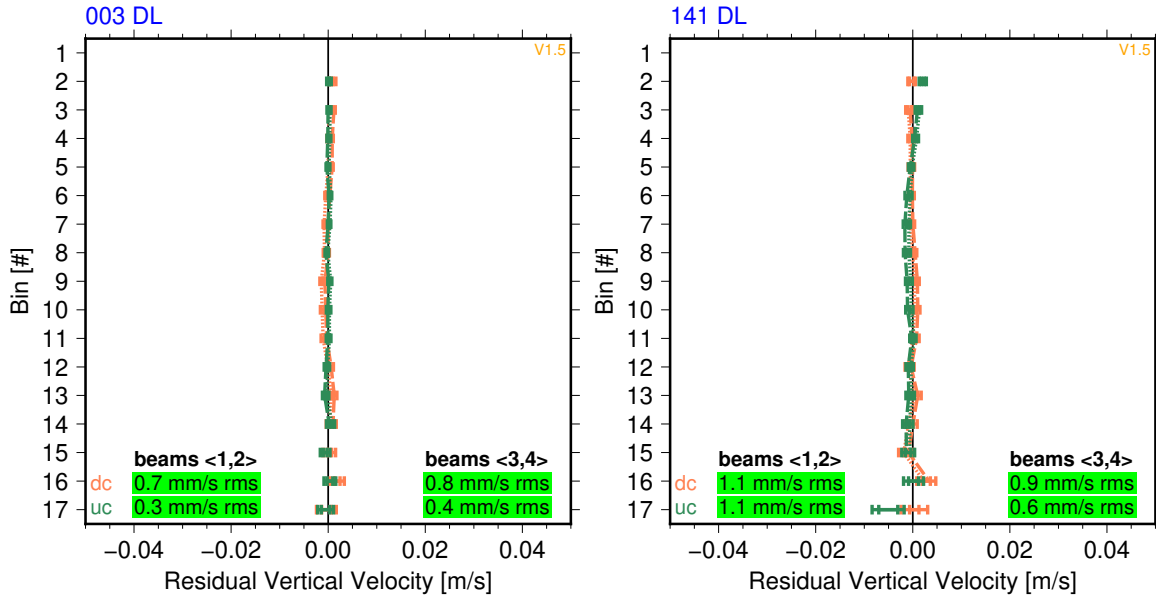
Figure 3: Example _bin_residuals.ps diagnostic plots for the two profiles of Figure 2. Each panel shows the mean residuals (with standard deviations) plotted against bin number (distance from ADCP transducer). The dc and uc labels printed inside the panel list downcast and upcast *rms* mean residuals in the block of bins with the best data (solid orange and green lines in the profiles); green, yellow and red background colors indicate data of progressively inferior quality; the same colors are used for the four small squares in the lower-right corner of the _wprof.ps plots (e.g. Figure 2).

DL/013_bin_residuals.ps This diagnostic figure shows the magnitude of the average vertical velocity residuals vs. distance from the ADCP transducer (bin number; Figure 3). Next to the profile summary plot, this is the most useful plot for diagnosing data problems. In particular, the residuals should be small and associated with little vertical structure. For both down- and upcast *rms* values of the mean-residuals in a block of high-quality ADCP bins (indicated by the orange and green lines in the profiles) are printed inside the figure panels over a background of green, yellow or red, indicating progressively worse data quality. In profiles with large vertical velocities, comparatively larger residuals can be tolerated than in more quiescent regions. The four "quality colors" of these plots are also shown as colored squares in the _wprof.ps diagnostic figures.

DL/013_residual_profs.ps This diagnostic figure shows profiles of vertical-velocity residuals from the two separate beam-pair estimates (Figure 4). This plot is useful for detecting anomalies affecting a particular part of the water column (e.g. due to biology near the surface, previous-ping interference, depth ranges with weak backscatter, . . .) or in a particular beam pair (e.g. due to package-wake effects). Anomalies indicating increased uncertainty near the seabed and the surface are commonly observed. The information from this diagnostic plot is used for the red hashing underlying the vertical velocity profiles in the _wprof.ps diagnostic figures.

DL/013_time_lags.ps Time series of lag-correlation offsets used to merge the LADCP to the CTD data (Figure 5). This plot is useful to verify that time-lagging was performing as intended and to diagnose dropped CTD scans (Appendix B.1).
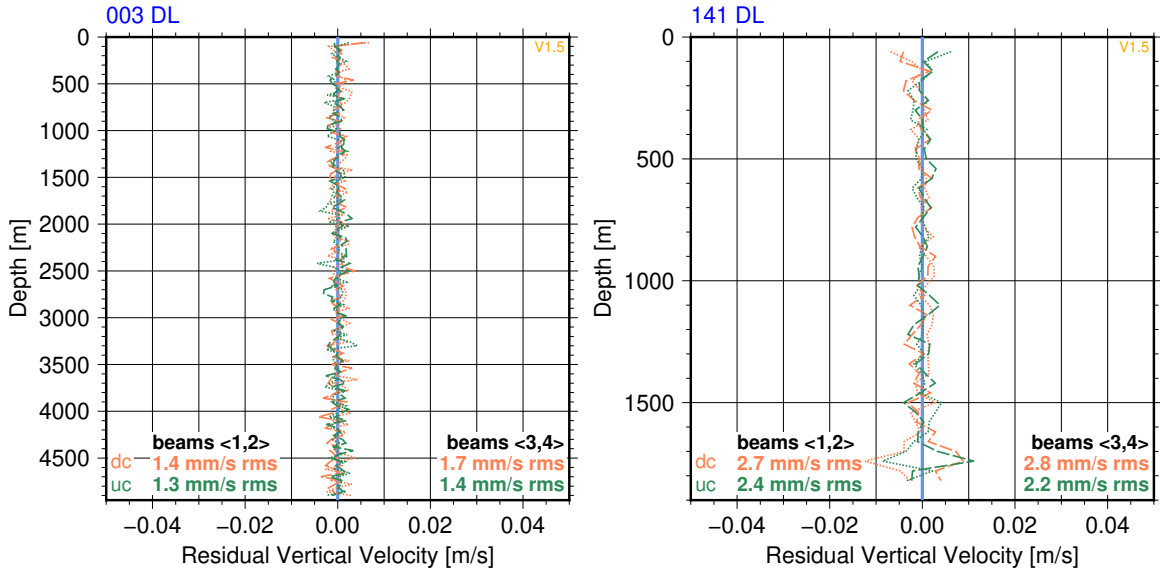
Figure 4: Example _residual_profs.ps diagnostic plots for the two profiles of Figure 2. Each panel shows profiles of mean beam-pair (dashed/dotted for beams <1,2>/<3,4>) and vertical-velocity residuals from the down- (orange) and upcasts (green). The overal *rms* values are printed inside the figure panels. Depth layers with anomalously large residuals are marked with red hashing in the _wprof.ps plots (e.g. Figure 2).

3.4   Processing Errors

Occasionally, data processing with LADCP_w_ocean fails with an error. The most common problem is that the automatic time-lagging algorithm fails to determine an unambiguous offset between the LADCP and CTD time series. Often, such time lagging problems can be corrected by manually determining an approximate time lag before processing, as follows:

1. Process the data with zero time lagging (-i 0 -u) and with the "quick-and-dirty" (-q) option. This should always produce a .tis time-series output file.

2. Using the .tis file, match the time series of LADCP_reflr_w to the time series of CTD_w by determining Δt so that CTD_w plotted against elapsed agrees with LADCP_reflr_w plotted against elapsed+Δt. Usually it is sufficient to estimate Δt to within 10 seconds or so.

3. Re-process the data with LADCP_w_ocean using the -i command-line option (or the variable $initial_time_lag in the processing configuration file) to set the initial time-lagging guess to Δt. (The -u option must not be used for this step.)

For dual-head LADCP systems, time-lagging problems are often restricted to one of the instruments. In this case, the CTD time lag from the instrument without the problems, which is reported in the metadata of the corresponding .wprof output file, can usually be used to set the initial guess (with the -i command-line option). When neither of these methods work, i.e. when time lagging fails even when a valid estimate for the initial guess is provided, time lagging must be carried out manually to within 1/24 s using the data from the .tis file, with the resulting lag supplied with the -i and -u options for processing.
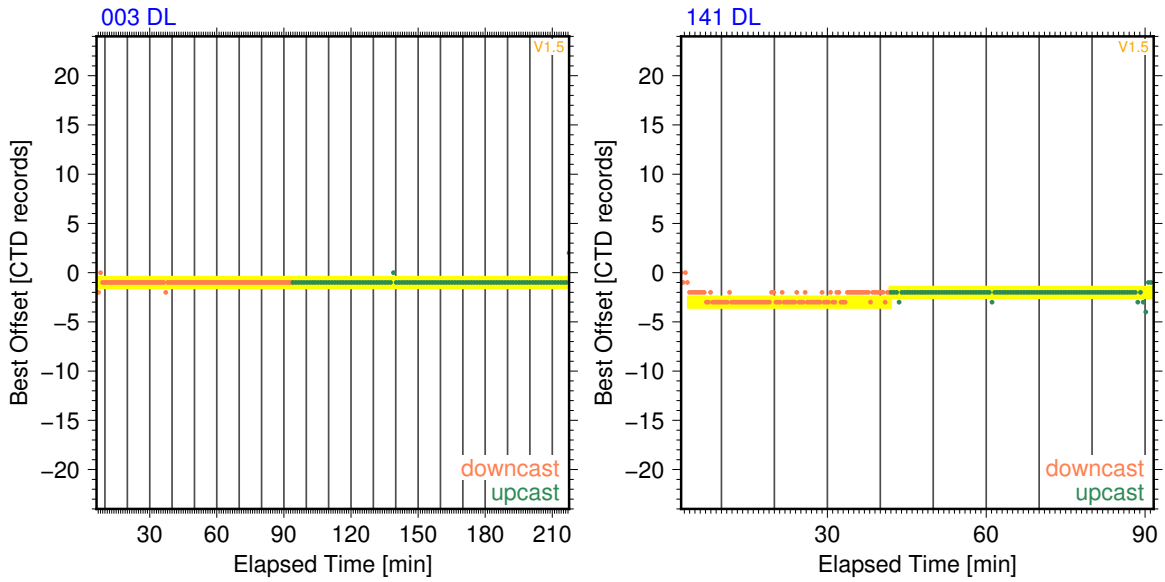
Figure 5: Example ⎵time⎵lags.ps diagnostic plots for the two profiles of Figure 2. Each panel shows a time series of the lags required for optimally matching the CTD to the ADCP data. Orange/green indicate downcast/upcast data; yellow bands underlie periods that have passed time-lag filtering. [Time-lag filtering and plotting of the yellow bands is disabled for CTD data that have been corrected for dropped scans (Section 2).]

In addition to time-lagging problems, there are many other error messages. While most errors are fatal and cannot be corrected some profiles with errors can be processed by relaxing some of the default data editing and filter parameters. Great care must be taken when interpreting such "force processed" profiles, which are likely associated with elevated errors.

17

4 Data Editing and Postprocessing (`LADCP_w_postproc`)

In most cases, the profiles of vertical ocean velocity derived with `LADCP_w_ocean` from the data from a single ADCP (Section 3) are suitable without further treatment as input for the finestructure VKE-based parameterization of kinetic energy dissipation described below (Section 5). However, post-processing of the vertical velocity data can be advantageous and is required in some cases:

- Vertical velocity measurements from TRDI ADCPs are associated with biases of a few $mm \cdot s^{-1}$. For deep profiles, cast-averaged vertical velocities are a good estimate for these biases, which should be subtracted from the measurements when absolute vertical velocity is required. For variance-based analyses, such as the VKE parameterization, bias correction is not required.

- LADCP profiles collected with dual-head systems *(Visbeck, 2002)* provide two, largely independent, w_{ocean} profiles per cast. For profiles with strong vertical velocity signals the data from the two ADCPs can be combined to improve the estimates, but the resolved vertical velocity signal in many open-ocean profiles is of the same magnitude or smaller than the measurement accuracy, implying that the data should not be combined for the analyses. However, since the diagnostic figure from the combined data is usually the easiest way for quickly assessing the quality of the processed velocities, it is recommended that this step is carried out for all profiles collected with a dual-head setup.

- Every processed w_{ocean} profile is contaminated by "random" measurement errors that include the effects of measurement noise and glitches (e.g. due to fish swimming across an ADCP beam), low backscatter (short range) and winch-velocity dependent errors, which can cause false apparent finestructure[10] associated especially with bottle stops during upcasts.[11] Data that are obviously bad should be removed before the profiles are used.

- During post-processing the vertical velocity samples (`.wsamp` files) are re-binned into vertical profiles. This re-binning can be done at a different vertical resolution from the original processing, either to increase the vertical resolution or to improve the signal-to-noise ratio. The re-binning can furthermore be carried out with the data from a sub-range of the ADCP bins.

These post-processing tasks can be carried out with the `LADCP_w_postproc` utility, which is described in the remainder of this section.

4.1 Bias Correction and Re-Gridding

In most locations and at most times the vertically averaged vertical velocity in the ocean is expected to be very close to zero. Averaged vertical velocities deviating from zero are therefore assumed to be dominated by instrument biases typically measuring several $mm \cdot s^{-1}$ (Section 3.3.1). Figure 6 shows example profiles from two different data sets with apparent upcast downwelling biases of about $1.5\,cm \cdot s^{-1}$, whereas the downcast velocities are apparently nearly unbiased. The mean instrument angles in both profiles are uncomfortably large, and both profiles have large upcast ADCP-bin-averaged velocity residuals (yellow squares in lower row).

Before re-gridding the data into a depth profile, `LADCP_w_postproc` subtracts the vertically averaged cast velocities, reported as "mean w" in the `_wprof.ps` summary plots, from the measurements.

---

[10]The vertical scale of these winch-velocity-related finestructure artifacts is limited by the vertical range of the ADCPs. In a data set from the East Pacific Rise vertical-wavenumber spectra of w_{ocean} indicate that vertical wavelengths shorter than $\approx 150\,m$ are significantly degraded by bottle-stop artifacts; shorter wavelengths were therefore not used in the analysis of *Thurnherr et al.* (2015).

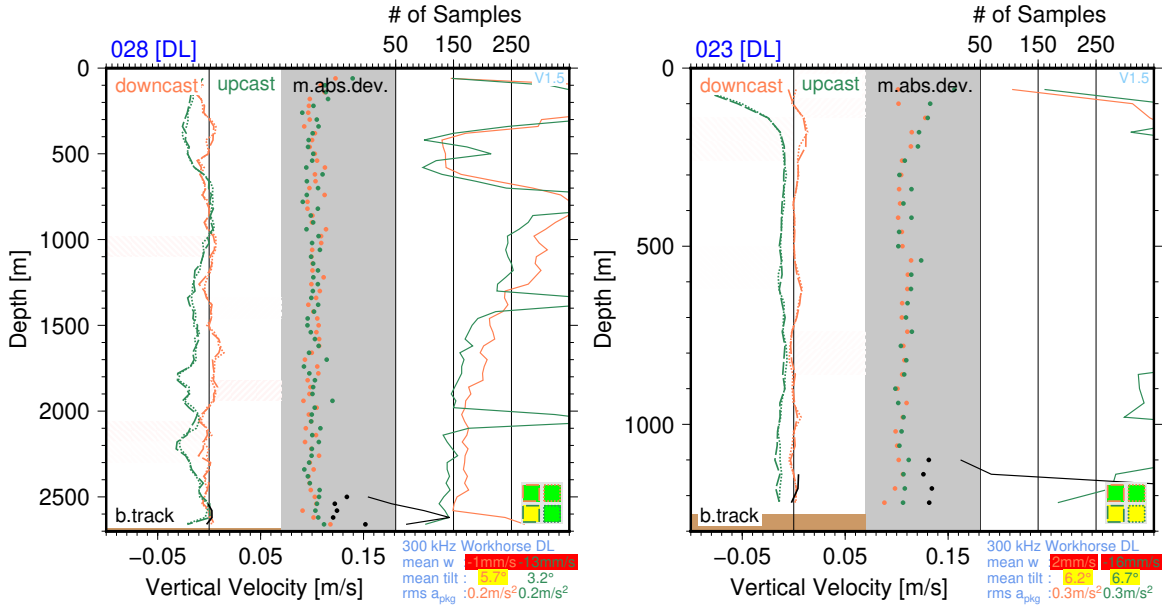[11]Any change in winch velocity, rather than just bottle stops, can be associated with vertical-velocity artifacts.

Figure 6: Example _wprof plots from two data sets associated with apparent downcast-/upcast vertical velocity biases. Left panel: East Pacific Rise crest; upcast velocities (green) are biased low by about $1.3\,\mathrm{cm\cdot s^{-1}}$. Right panel: Gulf of Mexico; upcast velocities are biased low by $\approx 1.6\,\mathrm{cm\cdot s^{-1}}$.

Therefore simple, empirical bias correction is achieved simply by feeding a .wsamp output file from LADCP_w_ocean to LADCP_w_postproc, e.g.

        LADCP_w_postproc DL/028.wsamp

This will creates both an output file 028.wprof and a diagnostic plot 028_wprof.ps in the working directory. By default the post-processed output is gridded with the same parameters (resolution and minimum number of samples) that were used for the original processing. The gridding parameters can be modified with command-line parameters. The following example creates a profile at 20 m vertical resolution *without* applying the bias correction:

        LADCP_w_postproc -z -o 20 DL/028.wsamp

This profile can be plotted together with the original profile (DL/028.wprof) for a direct comparison without any offset.

4.2 Combining Data from Dual-Head LADCP Systems

In dual-head LADCP systems, a given depth is sampled by two ADCPs at different times. During dowcasts, the depth is first sampled by the downlooker, starting at the farthest bin. Then, after a gap of a few seconds, the depth is sampled by the uplooker, starting at the nearest bin. As a result, the two ADCPs provide almost completely independent estimates of the oceanic w field, which can mostly be considered steady during sampling[12]. For profiles with equally excellent performance of

---

[12]With typical winch speeds of 50–60 meters per minute and valid velocity measurements between 10 and 150 m from the transducers a given depth layer is first sampled by the downlooker for about 2 min, before it is not sampled at all for
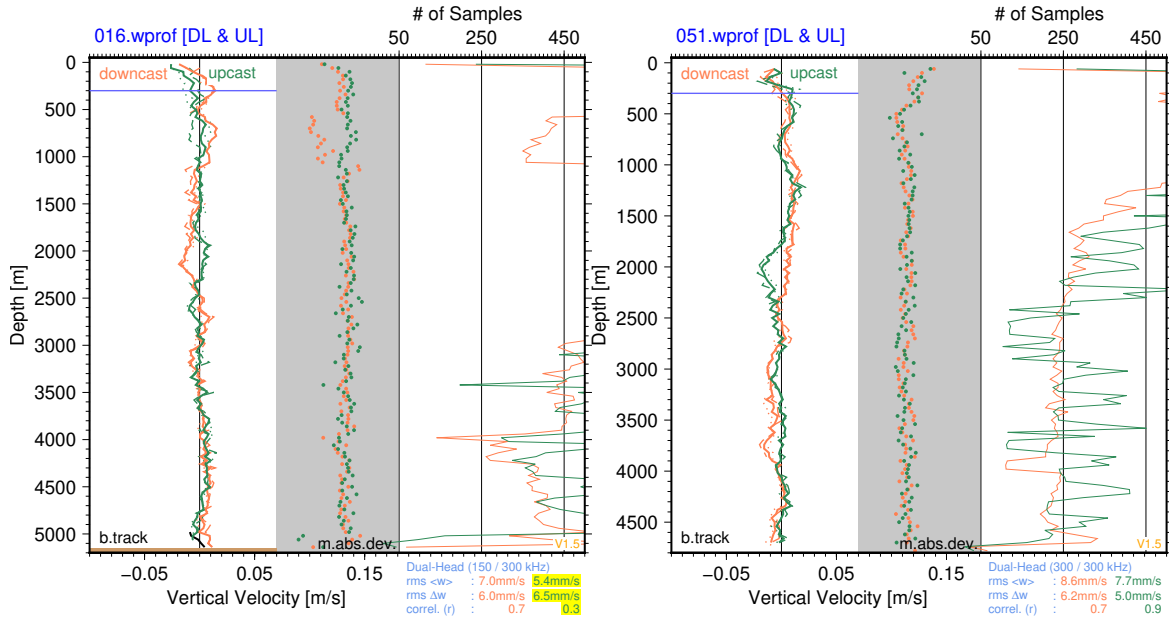
Figure 7: Example _wprof.ps diagnostic plots produced by LADCP_w_postproc from two recent profiles from the western North Atlantic (2021 GO-SHIP A20). The format of these plots is similar to the summary plots produced by LADCP_w_ocean (Figure 2), with the summary (on the right below the panels) listing per-cast rms(w_{ocean}) (the vertical velocity signal), the *rms* difference between the two single-instrument estimates (the overall accuracy), as well as correlation coefficients. Yellow background is used for cast where the signal is below the accuracy. Data from the near-surface layer (above the blue lines) are excluded from these statistics.

both ADCPs and/or with strong vertical velocity signals the data from the two instruments can be combined to yield improved profiles with smaller errors.[13] However, even after bias correction the differences between the velocity estimates from the two ADCPs in many open-ocean profiles is of the same magnitude or larger than the resolved vertical velocity signal, implying that the vertical profile derived from the data data from the two ADCPs should not be used for analysis.

In spite of this *caveat* the data from dual-head ADCPs should always be combined during quality control, mainly because the resulting diagnostic figure provides for an easy-to-interpret visual assessment of the data quality of the profile. In the example,

    LADCP_w_postproc DL/120.wsamp UL/120.wsamp

about 20 s, and then sampled again for 2 min by the uplooker. Since the measurement errors of the individual w_{ocean} estimates are dominated by the surface-wave related vessel heave with typical time scales on the order of 10 s, which is short compared to the gap length, the gap ensures statistical independence of the processed uplooker and downlooker samples. The total time of sampling is about 4 min, which is short compared to the buoyancy period except in the strongly stratified upper ocean (typically in the upper 200–300 m).

[13]It is important to note, however, that there are errors that are correlated between the down- and uplooker data. In particular, down-upcast bias differences such as the ones shown in Figure 6 are often observed in the data from both ADCPs in dual-headed systems. This implies that these biases are most likely due to errors in the w_{CTD} estimates. The acceleration dependency of the Paros Scientific pressure sensors used in SBE 911plus CTDs provides a likely source for these errors, and a possible explanation for the observation that upcast w_{ocean} profiles are sometimes (often?) better than the corresponding downcast profiles.

the DL and UL `.wsamp` files profile 120 are combined with `LADCP_w_postproc` to create a combined w_{ocean} profile (`120.wprof`), as well as a diagnostic plot (`120_wprof.ps`, Figure 7). The profile output from `LADCP_w_postproc` is similar to the the `.wprof` output from `LADCP_w_ocean`, except that there are no bottom-track and 2-beam solutions. The diagnostic figure has the same layout as the `_wprof` diagnostic plots produced by `LADCP_w_ocean` (Figure 2); when two input files are used, the individual profiles are plotted with thin dashed and dotted lines, respectively, and the combined profile is plotted with heavy solid lines. In order to add the BT profile to the plot, a downlooker `.wprof` file can be supplied with the `-b` command-line option. Listed on the right below the figure panel is the following summary information: i) Instruments; ii) *rms* ocean velocity in the combined profile (the vertical velocity signal); iii) *rms* difference between the two single-instrument estimates of w_{ocean} (the overall accuracy of the measurements); iv) per-cast correlations between the velocities (an indicator of the overall signal-to-noise ratio). Note that the data near the surface are excluded from these statistics.

4.3 Manual Data Editing

`LADCP_w_postproc` also provides a mechanism for manual editing of bad data. In many cases the bad data to be removed can be found quite easily by inspecting the diagnostic plots produced during data processing. As additional help, some of the problems commonly encountered with automatically processed vertical velocity profiles are listed in appendices B.1–B.6. Data editing instructions for `LADCP_w_postproc` are provided in a file called `./EditParams`, a `perl` script that is executed for each of the `.wsamp` files. (Note that `./EditParams` is executed twice when combining the data from dual-headed LADCP systems into a single profile.) There is a small library of data-editing functions:

`output_resolution(20);` This statement sets vertical output resolution to 20 m, which is appropriate for data collected in a region with strong acoustic backscatter. By default, the output resolution is taken from the input files (i.e. it is set by `LADCP_w_ocean`). Alternatively, it can be set with the `-o` command-line option to `LADCP_w_postproc`.

`bad_range_uc("depth",3700,"*");` Exclude the upcast vertical velocity data between 3700 m and the seabed from the gridded output profiles. The first argument can be any field name from the `.wprof` input file(s). Any number of "bad ranges" can be defined. The functions `bad_range_dc()` and `bad_range()` are also defined; the latter defines a common range for both downcast and upcast data.

In order to apply data editing only to specific profiles and/or run labels the editing functions must be made conditional with `if`-statements using the variables `$PROF` and `$RUN` as shown in the `ProcessingParams` example in Section 3.2. The following code example excludes the uplooker downcast data from processing of all profiles between 20 and 30:

```
if ($PROF>=20 && $PROF<=30 && $RUN eq "UL") {
    bad_range_dc("depth","*","*");
}
```

5 Calculating Finescale VKE and ϵ_{VKE} (`LADCP_VKE`)

5.1 Preliminary Comments

Nearly everywhere instantaneous w_{ocean} is dominated by high-frequency (near the buoyancy frequency N) internal gravity waves. As the typical magnitude of internal-wave related vertical velocities ranges from mm·s^{-1} to cm·s^{-1}, LADCP data are particularly suitable in principle for estimating internal-wave VKE. To quantify total VKE, vertical-wavenumber (k_z) spectra derived from the w_{ocean} profiles must be integrated over the entire internal-wave wavenumber range. This is not usually possible, because the long-wavelength cutoff of the internal-wave range is not known. However, observations covering a wide range of environmental parameters (latitude, density stratification, Turner angle, water depth, . . .) and dynamical regimes (equatorial thermocline, Drake Passage, Luzon Strait, open abyssal ocean, . . .) show that finestructure VKE density $\propto k_z^{-2}$, and that the VKE density level is $\propto \epsilon$ *(Thurnherr et al., 2015)*. The software described here carries out all the manual data editing described in the paper automatically, producing results that are consistent not only with the original microstructure data sets but also with more recently acquired ones.

The k_z^{-2} dependence of the VKE spectra implies that total VKE is dominated by large vertical scales, emphasizing the problem of not knowing the large-wavelength cutoff required for spectral integration. However, the universality of the VKE vertical-wavenumber power law allows well constrained estimates of VKE density in the internal wave band by fitting the power law to observed spectra and sampling the fitted function at an arbitrary wave number. In *Thurnherr et al.* (2015) the VKE power levels are quantified by p_0 [in units of m^2·s^{-2}·(rad/m)$^{-1}$], the intercept of the power-law fit carried out in log-space, i.e. p_0 is the VKE density at wavenumber $1\,\text{rad·m}^{-1}$.[14]

5.2 Calculating p_0 and ϵ_{VKE} with `LADCP_VKE`

In order to calculate p_0 and apply the VKE finestructure parameterization for turbulent dissipation (ϵ_{VKE}) the utility `LADCP_VKE` is provided. As input, it takes one or two `.wprof` files, created either with `LADCP_w_ocean` (Section 3) or with `LADCP_w_postproc` (Section 4.3). *When both DL and UL data are available, the two single-head .wprof files should be used as input to LADCP_VKE, rather than the combined profile derived with LADCP_w_postproc (Section 4.2).* By default `LADCP_VKE` produces a `.VKE` data file, as well as a diagnostic plot (`_VKE.ps`). `LADCP_VKE` splits each profile into *windows* for calculating the spectra. For each spectral window, the output data files produced by `LADCP_VKE` contain the following fields:

widx Index of spectral window, counting downward from 1 near the surface; an additional bottom window (see below) has `widx = -1`.

depth, depth.min, depth.max Center depth of the window in meters, as well as upper and lower window limits.

hab Distance of the window center from the seabed. This field only contains numeric values when the water depth is known. For full-depth DL profiles this is typically the case, but for profiles where the water depth cannot be determined automatically, it must be supplied with the `-h` option to `LADCP_w_ocean` (Section 3).

---

[14]This wavenumber corresponds to a vertical wavelength of $6.3\,\text{m}$, which can cause confusion because it is too short to lie inside the finestructure (internal-wave) range. While this fact does not matter, confusion can easily be avoided by sampling VKE density at a different wavenumber. For example, $p_{\text{fs}} = p[k_z = 0.1\text{rad}m^{-1}] = 100 \times p_0$ may be more palatable for plotting than p_0 as it represents VKE density at wavelengths of $\approx 65\,\text{m}$, well within the expected internal-wave range.

nspec Number of w_{ocean} profiles used to determine each spectrum. E.g. for VKE profiles derived from both down- and upcast data from dual-head ADCP systems, `nspec = 4`, except where there are long gaps in any of the profiles. Maximizing the number of independent samples is the main reason the two single-head LADCP output files should be used to estimate VKE from profiles collected with dual-head systems.

w.nsamp.avg For each input file the median number of w_{ocean} samples in the input data used to calculate the spectra is calculated. (The median is used to avoid biasing the estimates by bottle stops.) `w.nsamp.avg` is then set to the average of these medians.

pwr.tot, pwr.fs VKE power integrated across the entire spectrum and across the finestructure wavenumber range, respectively. Note that these powers are not corrected, e.g. for removal of the means.

p0 In order to determine the VKE power density, a k_z^{-2} (fixed-slope) power-law is fit to the spectral power in each window. The parameter p_0 is the value of the resulting power-law fit sampled at $k_z = 1\,\mathrm{rad\cdot m^{-1}}$.

p0fit.rms, p0fit.r, p0fit.slope, p0fit.slope.sig Fitting the k_z^{-2} power law to the observed spectra provides a set of statistics: `p0fit.rms` is the *rms* discrepancy between observed VKE and the best-fit k_z^{-2} power law; `p0fit.r` is the correlation coefficient (in log-log space) of finestructure VKE density vs. vertical wavenumber; `p0fit.slope` and `p0fit.slope.sig` provide the best-fit (least-squares) power-law slope.

eps.VKE This field contains the primary result from the VKE-finestructure-parameterization for kinetic energy dissipation in units of $\mathrm{W\cdot kg^{-1}}$. The field only contains numeric values for the windows meeting all of the following, mutually consistent, criteria:

1. The profile was collected poleward of $3°$ of latitude. The cutoff latitude is an estimate based on inspection of plots from the 2015 US GO-SHIP P16N cruise.

2. The k_z^{-2} spectral fit in log-log space has an *rms* misfit `p0fit.rms <= 0.4`. This filter was found by *Thurnherr et al.* (2015) to maximize the overall agreement between VKE and microstructure in their data.

3. `w.nsamp.avg` ≥ 50. The limiting value for this filter was derived from the data of multiple cruises in regions of weak backscatter, where it corresponds approximately to `p0fit.rms <= 0.4`.

4. The power-law slope derived from the least-squares fit in log-log space must be approximately equal to -2 (`p0fit.slope` between -3 and -1; this range of slopes corresponds approximately to `p0fit.rms <= 0.4`).

5. Spectral power and wavenumber are significantly correlated (`p0fit.r <= -0.4`). This cutoff corresponds approximately to `p0fit.rms <= 0.4`.

The additional filter criteria (3–5), which were not used in the analysis of Thurnherr et al. (2015), primarily remove estimates with low ϵ_{VKE}. These erroneous low-ϵ estimates biased both curve fits used to determine empirical scaling constant c in the original analysis identically, resulting in a uniform (independent of turbulence level) high-bias of the parameterization. Bias of the same magnitude is observed with an additional data set that had not been included in the original analysis (DIMES UK2). In order to correct for this bias the scaling constant, which is recorded in the metadata of the output files, was increased by 21% to $0.026\,\mathrm{s}^{-\frac{1}{2}}$.

By default, the VKE spectra are calculated in half-overlapping windows neither exceeding 32 samples nor 600 m vertical wavelength. (For profiles binned at the default 40 m resolution, 320 m-thick windows are used by default.) Data from a 150 m-deep near-surface layer are ignored by default, which implies that the center depth of the top window is typically at 310 m. In order to avoid unnecessary bottom gaps, an additional window is created near the seabed[15] — note that this bottom window overlaps more than 50% with the window above. By default, spectra are calculated from both downcast and upcast data and the results averaged, but there are `-d` and `-u` options that can be used to use downcast or upcast data alone. For dual-head profiles, the `-d` and `-u` options affect both input files. Before calculating the spectra, means are removed (changeable with the `-o` option), and the spectra are corrected for attenuation of the high wavenumbers due to depth-averaging by the instrument and during processing *(Polzin et al., 2002; Thurnherr, 2012)*.

Similar to LADCP-derived horizontal velocities *(Polzin et al., 2002)*, the effective vertical resolution of LADCP-derived w_{ocean} is much coarser than the bin length used to acquire the data. Deviations in VKE spectra from the apparently universal k_z^{-2} power law *(Thurnherr et al., 2015)* allow visual determination of the noise-cutoff wavelength from spectral plots. By default, `LADCP_VKE` uses a 100 m vertical-wavelength cutoff which is suitable for many typical LADCP data sets. The short-wavelength cutoff can be modified with the `-c` command-line option.

5.3 Quality Assessment

`LADCP_VKE` produces diagnostic plots that show both VKE spectra and derived ϵ_{VKE} profiles (Figure 8). Gaps in VKE profiles are very common. In general, the number of gaps tends to increase with decreasing VKE levels. High-quality profiles have fewer gaps than profiles associated with measurement problems. By far the best way to validate VKE-derived turbulence levels is by comparison with simultaneous microstructure profiles. When such profiles are available they can be supplied as input with the `-k` command-line option to `LADCP_VKE`, which adds the microstructure data, averaged in the same way as the VKE estimates, to the diagnostic plots (e.g. right figure panel).

When no microstructure data are available, the overlapping spectral windows allows a simple visual assessment of the profile consistency. In case of the example profile shown in the left panel of Figure 8, the scatter of the ϵ_{VKE} estimates indicates that the (weak) turbulence levels below 2000 m are not tightly constrained by individual spectral estimates, which implies that additional averaging is required to improve the signal-to-noise ratio.

In general, heavy averaging is required for reducing the noise associated with the generally lognormal intermittency of any turbulence data. For heavily averaged data separate VKE estimates can be derived from the down- and up-cast data, and from the two ADCPs in dual-headed LADCP systems. Figure 9 shows this idea applied to the cruise-average ϵ_{VKE} profiles from the 2021 occupation of the A20 repeat-hydrography section, consisting of 90 profiles. The four largely independent profiles show vertically uniform turbulence levels of $\approx 10^{-10}\,\mathrm{W\cdot kg^{-1}}$ below 2000 m, and approximately exponentially increasing turbulence above, apparently reaching levels between 10^{-9} and $10^{-8}\,\mathrm{W\cdot kg^{-1}}$ near the sea surface.

---

[15]Unless the `-b` command-line option is used

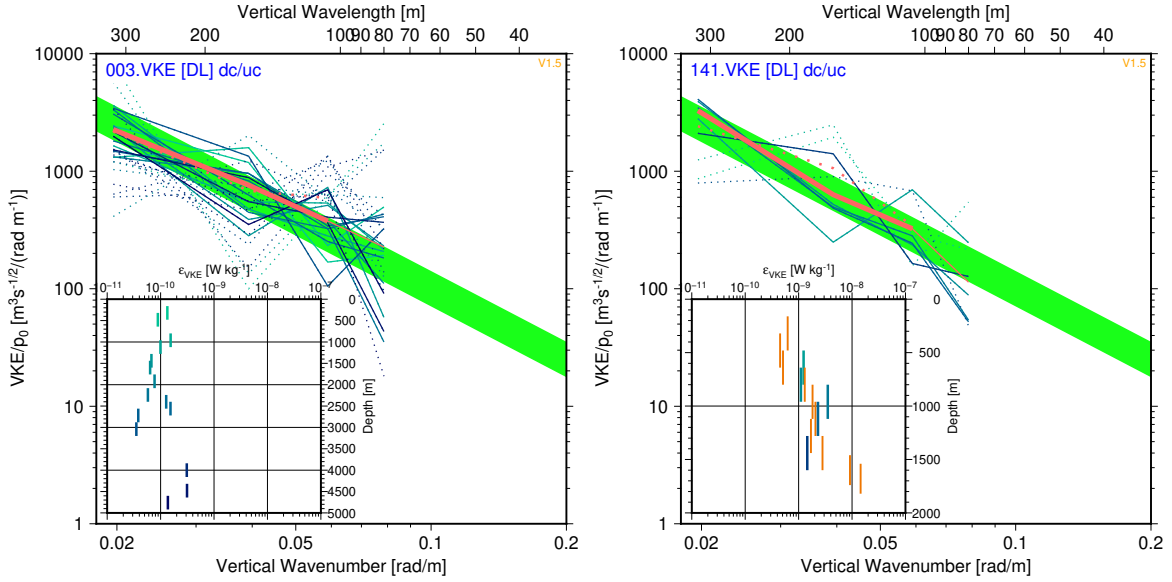Figure 8: Example _VKE.ps diagnostic plots from DIMES US2 cruise with weak (left panel) and strong (right panel) vertical velocities (same profiles as used in Figure 2). Samples from each window are plotted in blue, with darker shades indicating deeper depths. Main panels: p_0-normalized VKE spectral density vs. vertical wavenumber; individual window spectra are plotted in blue, with dots indicating spectra that do not pass the tests required for estimating ϵ_{VKE} (Section 5.3); solid and dotted pink lines show mean spectra calculated from only the good and from all window spectra, respectively; the finestructure ranges used for the spectral fits are marked with the heavy line of the mean spectra (100–320 m in these cases); the mean finestructure spectra should lie entirely on top of the green-shaded areas, which encompass factor-2 uncertainties in the derived ϵ_{VKE} estimates. Insets: ϵ_{VKE} derived from the VKE spectra that pass the quality checks (blue), and $\epsilon_{\mu s}$ from a simultaneous velocity microstructure profile (orange; not available for profile 003).

A   Alternative CSV File Format For CTD Data

The preferred formats for CTD time-series data are binary or ASCII SBE CNV files, because they contain useful meta-data. The simple ASCII CSV (comma-separated values) format described here allows for fewer consistency checks and, therefore, requires additional care. The following assumptions are made for CSV ASCII CTD time series files:

1. 24 Hz sampling frequency

2. pressure in units of dbar

3. temperature in units of °C using ITS-90

4. conductivity in units of mS·cm^{-1}

Each CSV ASCII CTD file has a single header line listing the latitude, longitude and, optionally, the number of the profile, followed by the data records with scan number, pressure, *in situ* temperature and conductivity. Scan numbers must be consecutive and start at 1. Missing values are allowed, but
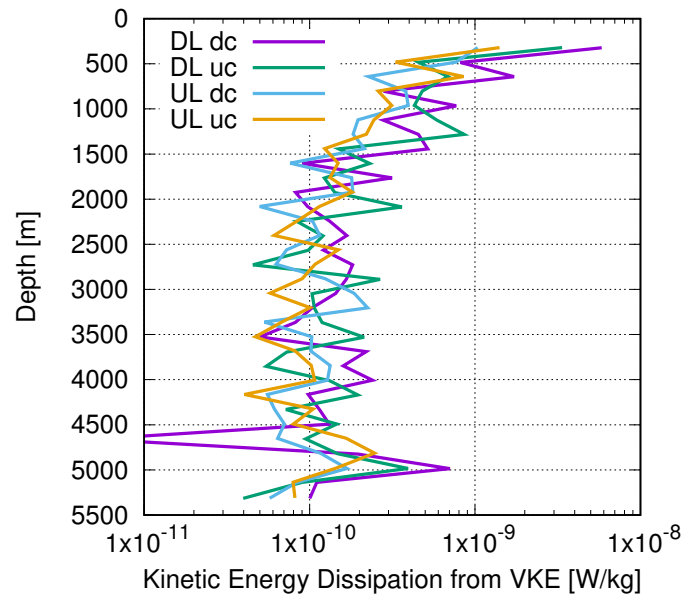
Figure 9: Ensemble averaged ϵ_{VKE} profiles from the 2021 occupation of the A20 repeat-hydrography section. DL and UL indicate dowlooker- and uplooker-only profiles; dc and uc indicate down- and upcast-only profiles.

comments and empty lines are not. The following shows the beginning of an example CSV ASCII CTD file with station number (7) and two missing values:

```
-53.939,86.57,7
1,12.525,3.8788,31.499201
2,12.433,3.8789,
3,12.468,3.8788,31.499325
4,12.419,,31.499388
5,12.489,3.8788,31.499013
6,12.419,3.8788,31.499075
```

B   Common Data Problems

Most of the plots in this appendix were produced with older versions of the processing software and some look somewhat different from plots produced with the current software version. The software version used to produce the plots is indicated in the top right corners in most of the figure panels.

B.1   Dropped CTD Scans

As described in Section 2 data transmission problems in SBE 911plus CTD systems cause dropped scans, which can be corrected for as long as the all required fields are archived in the 24 Hz time-series files. When this is not the case, gaps must be dealt with during processing. As long as only one or two "scan-drop events" occur during a profile this problem is usually easily detectable in the `_time_lags` plots (Figure 10). Profiles with more than two "scan-drop events," on the other hand, usually cannot be processed with `LADCP_w_ocean` at all. In the example shown in the upper two figure panels three CTD scans (1/8 s worth of data) were dropped approximately 15 min after the beginning of the cast. As the pre-drop time lag is used for the downcast (solid line) the downcast data after the dropped scans are bad and are removed by the automatic editing. [Alternatively, the `-p` option of `LADCP_w_ocean` can be used to carry out "piece-wise" time lagging. By default, `LADCP_w_ocean` lags the downcast and upcast data separately.] In the example shown in the bottom two panels of the figure, the number of scans dropped was too great for the time-lagging algorithm to work correctly at the beginning of the cast.

B.2   Insufficient Sampling & Profile Gaps

Bad ADCP data, e.g. due to insufficient acoustic scattering or large instrument tilts, can cause insufficient sampling and, in extreme cases, gaps in the vertical-velocity profiles. While such data gaps are not problematic *per se* (Section 1), there are often vertical-velocity artifacts where the number of samples per depth bin is low, including at the edges of profile gaps, as well as near the sea surface and seabed. In the example shown in Figure 11, there are insufficient (<40, in this case) upcast samples in the following depth ranges: 186–196 m, 316–338 m, 356–368 m, 402–414 m, in addition to couple of isolated single-record gaps. At the edges of some of these gaps (e.g. just above 185 m in Figure 11, and also at both edges of the wake-affected upcast data gap shown in the right panel of Figure 12), there are clear artifacts that must be removed during post-processing. Alternatively, the gaps in this profile can be avoided altogether by processing (or post-processing) at a coarser vertical resolution.

B.3   Package-Wake Effects

It is a fairly common observation in LADCP work that uplooker downcast data and/or downlooker upcast data are affected by package wakes. In the context of vertical-velocity processing, these wakes manifest themselves as vertically coherent layers where the two independent 2-beam solutions for w_{ocean} disagree significantly. In the example shown in Figure 12 package-wake effects affect the upcast data between 50 and 100 m and, more importantly, the wake causes an erroneous apparent upwelling peak centered at 190 m in one of the two 2-beam upcast solutions, which must be removed during post-processing.

It is important to note that the difference between the two 2-beam solutions is identical (except for a scaling constant) to the so-called ADCP *error velocity.* Since error velocity is used as a data-editing criterion in `LADCP_w_ocean`, the most severely wake-affected samples are discarded automatically during processing, leading to gaps in the w_{ocean} profiles and gap-edge artifacts (Section B.2), which can be difficult to attribute to wake effects (right panel in Figure 12).
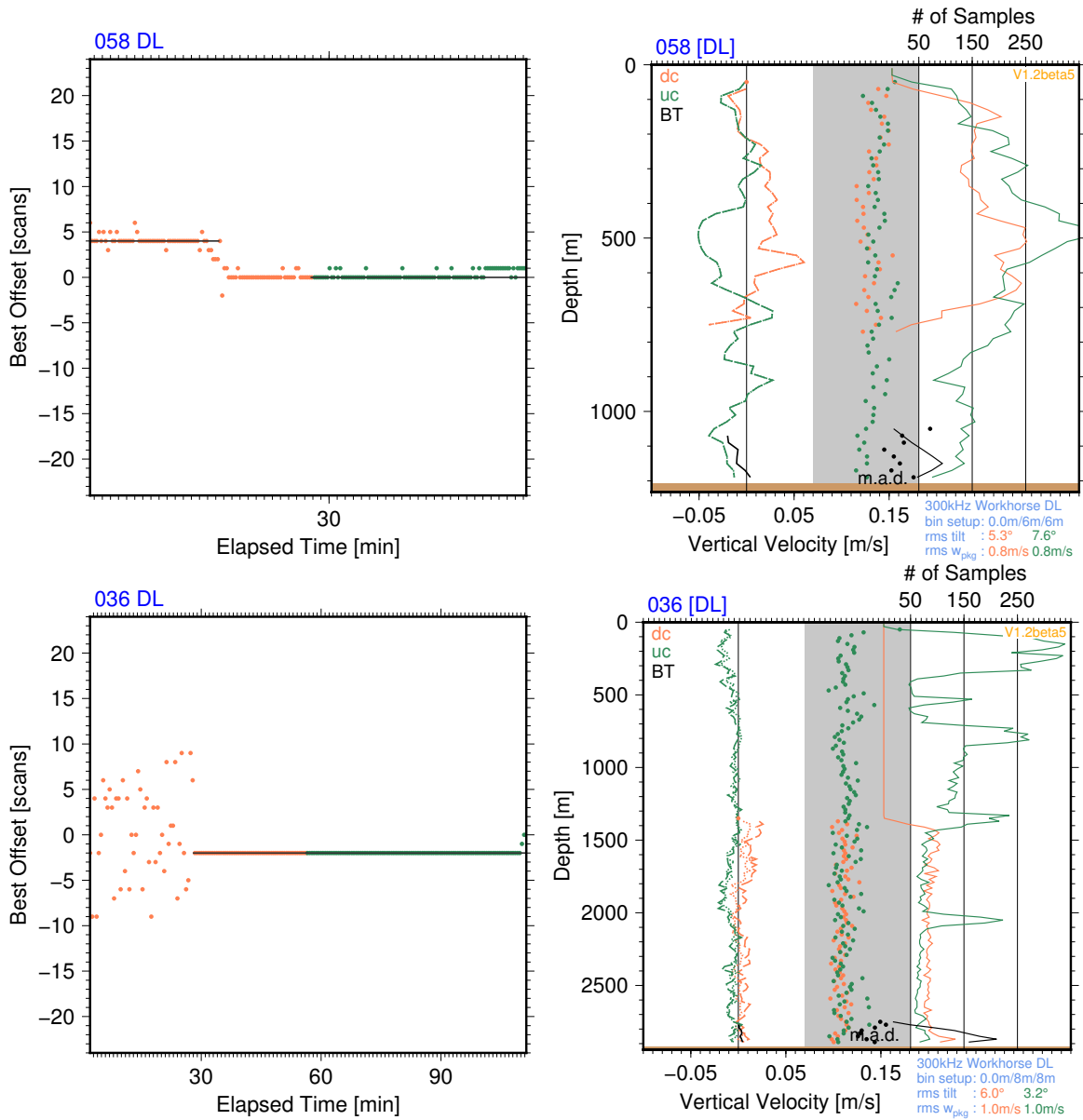
Figure 10: Diagnostic plots from two example profiles (upper and lower panels, respectively) with dropped CTD scans. Left panels: _time_lags plots. Right panels: _wprof plots.

B.4 Biology

Not all vertical motion measured by ADCPs near the sea surface is due to vertically moving water, as at least some of the organisms giving rise to the acoustic backscatter required for ADCP measurements are capable of rapid vertical movement. There are regions where vertical plankton migrations dominate upper-ocean ADCP vertical-velocity measurements at certain times of the day (e.g. *Fischer*
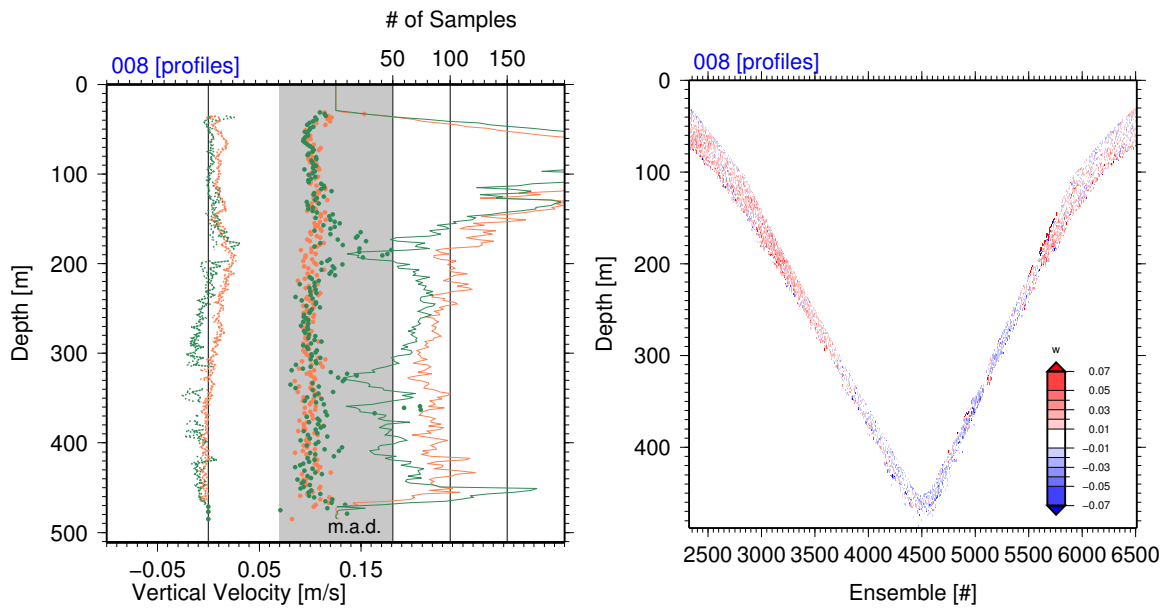
Figure 11: Diagnostic plots from a profile from the equatorial Pacific with insufficient sampling; software V1.1. Left panel: _wprof plot. Right panel: _wsamp plot.
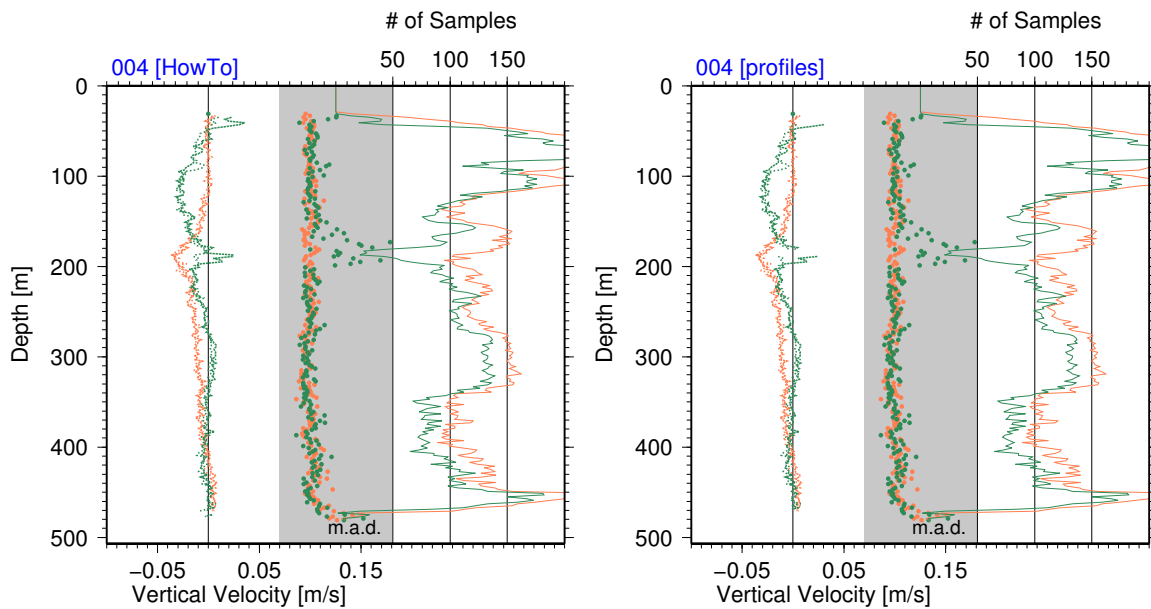

Figure 12: Diagnostic _wprof plots from an equatorial Pacific profile affected by package wake; software V1.1. Left panel: Profile processed with the requirement of ≥20 samples per depth bin. Right panel: Profile processed with the requirement of ≥40 samples per depth bin.
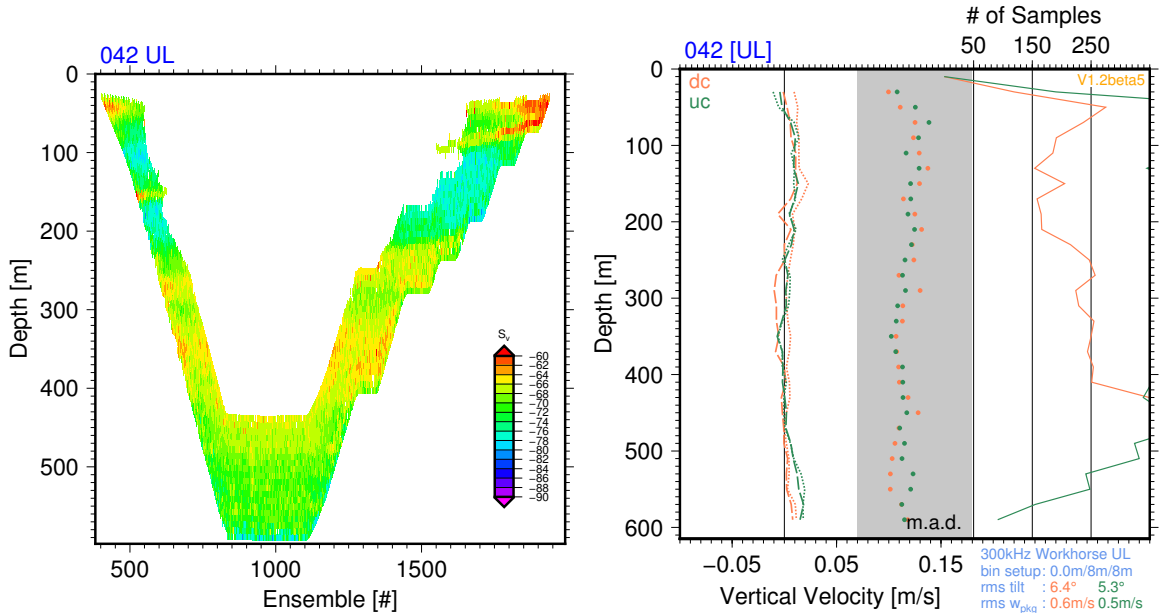
Figure 13: Diagnostic plots from a profile with a likely ≈10 m-thick layer of vertically moving plankton rising from 160 to 60 m during the cast; software V1.0. Left panel: _Sv plot; the anomalous vertical structure of acoustic backscatter below 400 m is due to imperfections in the backscatter calculation algorithm. Right panel: _wprof plot.

and Visbeck, 1993b). In the example shown in Figure 13 there is a likely ≈10 m-thick layer of upward-moving plankton rising from 160 to 60 m during the cast (left panel). While this vertically moving layer does not appear to affect the processed w_{ocean} profiles significantly (right figure panel) there are apparent downcast artifacts associated with another thin acoustic scattering layer near 160 m.

Vertical velocities in the upper ocean should generally be treated with particular caution, especially in regions of high biological productivity. In a data set collected in the northeastern Gulf of Mexico, for example, consistently strong apparently downward motion was observed in the upper 200 m in the profiles taken between sunset and sunrise, but not during daylight hours (Figure 14). While inconsistent with *diel* vertical plankton migration, the observed downward motion is associated with strong acoustic backscatter anomalies (middle panel), consistent with the hypothesis that the apparent motion is caused by swimming organisms. The consistent apparently downward motion can be explained by radially outward swimming organisms: Since vertical velocities are calculated as averages of the along-beam velocities from two opposing beams (Appendix C), radial outward motion results in a false apparent downward velocity. This error is due to the violation of the assumption of horizontal homogeneity of the velocity field that underlies ADCP velocity measurements.

B.5   Boundary Effects

In addition to biology, there are other causes for potential contamination near the sea surface, including reduced sampling, interference from acoustic instruments mounted on the surface vessel, sidelobe reflections from its hull and the sea surface, as well as high-frequency vertical motion associated with (long) surface-gravity waves. Near the seabed, reduced sampling and sidelobe reflections from steep
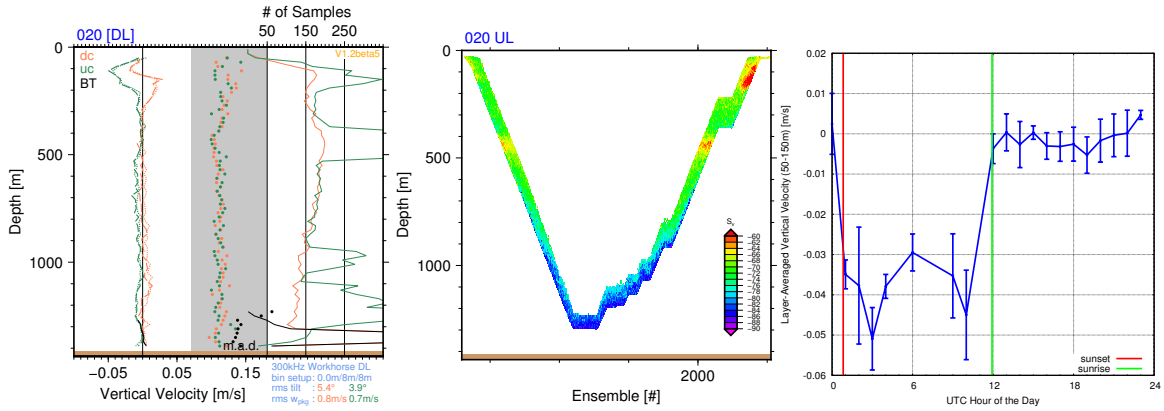
Figure 14: Upper-ocean vertical velocity signals in the northeastern Gulf of Mexico likely caused by biology. Left and middle panels: Diagnostic `_wprof` and `_backscatter` plots from an example profile with strong apparent downwelling observed during the upcast in the upper 200 m of the water column. Right panel: Average w_{ocean} between 50 and 150 m vs. hour of the day for all profiles from this site.
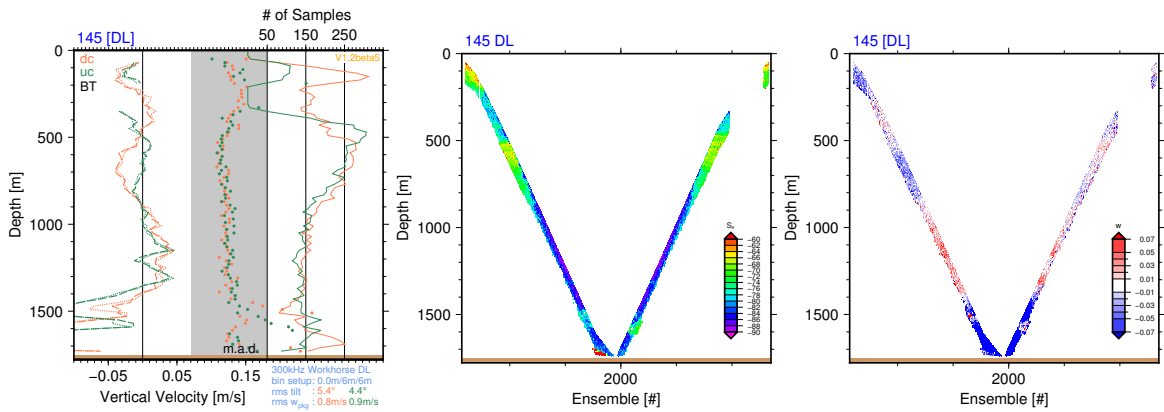

Figure 15: Diagnostic plots from a profile in a region with very strong turbulence. From left to right: `_wprof`, `_Sv` and `_w` plots, respectively.

topography can adversely affect the data. (When pinging simultaneously, sidelobe contamination from the seabed affects uplooker as well as downlooker data, which makes it important that the water depth is set correctly when processing uplooker profiles; Section 3.1.)

B.6 Strong Turbulence

High levels of turbulence in regions such as Drake Passage and Luzon Strait can affect LADCP-derived vertical-velocity profiles. The example profile shown in Figure 15 was collected slightly east of the crest of a meridionally trending ridge blocking deep flow through Luzon Strait. At the time of observation, there was strong eastward bottom-intensified flow at the location. Following the sloping topography, the eastward flow is associated with strong downwelling (left figure panel). Both the elevated acoustic backscatter between 1500 and 1600 m (center panel) and the bursts of upward

motion embedded within the strongly downwelling background (right panel) are consistent with the signatures of large turbulent eddies in this layer of extreme vertical shear of the zonal flow ($\approx 0.5 \, \mathrm{m \cdot s^{-1}}$ over $100 \, \mathrm{m}$). The vertical velocities associated with the turbulent eddies contaminate both downcast and upcast profiles of w_{ocean} (left panel).

C Coordinate Transformations

C.1 Beam-Coordinate ADCP Data

The following algorithm is used to derive vertical velocities from LADCP data acquired in radial beam coordinates:

1. Using linear interpolation, the along-beam velocities are re-sampled at the levels of the nominal bin centers

$$z_{\text{bin}} = z_{\text{ADCP}} + \Delta_{\text{bin}} \cos \tau, \tag{2}$$

where Δ_{bin} is the center-line (along the ADCP yaw axis) distance between the ADCP transducer and the bin center, and

$$\tau = \cos^{-1}(\cos \phi \cos \rho) \tag{3}$$

is the instrument tilt (deviation from the vertical), with ϕ and ρ denoting pitch and roll angles as measured by a set of gimbals aligned with beampairs <1,2> (ϕ) and <4,3> (ρ), respectively. TRDI ADCPs do not measure ϕ but, rather, ϕ_{RDI}, from which ϕ can be derived as follows *(RD Instruments, 1998)*

$$\phi = \tan^{-1}(\tan \phi_{\text{RDI}} \cos \rho). \tag{4}$$

2. The beam velocities (b_1, b_2, b_3, b_4) are transformed into the instrument coordinate system used by TRDI ADCPs *(RD Instruments, 1998)*: v'_{12}, v'_{43}, w'_{avg}, and e_{RDI}, where v'_{12} and v'_{43} are the quasi-horizontal[16] velocity components in the roll and pitch planes, respectively, i.e.

$$v'_{12} = \frac{b_1 - b_2}{2 \sin \beta} \tag{5}$$

$$v'_{43} = \frac{b_4 - b_3}{2 \sin \beta}, \tag{6}$$

with β denoting the transducer beam angle from the vertical, $w'_{\text{avg}} = (w'_{12} + w'_{34})/2$, with w'_{12} and w'_{34} denoting the two independent two-beam measurements of quasi-vertical velocity, i.e.

$$w'_{12} = \frac{b_1 + b_2}{2 \cos \beta} \tag{7}$$

$$w'_{34} = \frac{b_3 + b_4}{2 \cos \beta}, \tag{8}$$

and

$$e_{\text{RDI}} = \frac{b_1 + b_2 - b_3 - b_4}{2\sqrt{2} \sin \beta} \tag{9}$$

$$= \sqrt{2} \tan \beta (w'_{12} - w'_{34}) \tag{10}$$

is the TRDI "error velocity", which is scaled by ≈ 0.5 ($\sqrt{2} \tan \beta \approx 0.51$, for $\beta = 20°$) for convenient comparison with the horizontal velocity components *(RD Instruments, 1998)*.

3. The quasi-vertical velocities in instrument coordinates[17] (w'_{12}, w'_{34} and w'_{avg}) are rotated into a coordinate system where the vertical velocities are aligned with the gravitational vector,[18] using

---

[16]Ignoring instrument tilt.

[17]This does *not* include e_{RDI}, which is always reported in instrument coordinates.

[18]This system is sometimes called "horizontal coordinates" *(RD Instruments, 1998)*. It differs from earth coordinates in that the horizontal velocities are not corrected for heading.

the rotation matrix (A1) from *Lohrmann et al.* (1990) for data collected with downward-looking instruments (for which $w > 0$ implies upward velocity).[19] Specifically,

$$w = w' \cos \phi_c \cos \rho - v'_{12} \cos \phi_c \sin \rho + v'_{43} \sin \phi_c \tag{11}$$

with

$$\phi_c = \sin^{-1} \frac{\sin \phi \cos \rho}{\sqrt{1 - \sin^2 \phi \sin^2 \rho}}. \tag{12}$$

Note that while transformation expression (11) looks superficially identical to the one used by TRDI ADCPs *(RD Instruments,* 1998),

$$w = w' \cos \phi \cos \rho - v'_{12} \cos \phi \sin \rho + v'_{43} \sin \phi, \tag{13}$$

it is different in that the rotation angle in the pitch plane ϕ_c is more accurate than ϕ used in the TRDI instrument-to-earth transformation, with the errors increasing with increasing instrument roll.

C.2   Earth-Coordinate ADCP Data

For LADCP data acquired in earth coordinates, the transformation from beam to horizontal coordinates is carried out by the instrument firmware. In instrument coordinates,

$$w'_{12} = w'_{\text{avg}} + \frac{1}{2}(w'_{12} - w'_{34}) \tag{14}$$

$$w'_{34} = w'_{\text{avg}} - \frac{1}{2}(w'_{12} - w'_{34}). \tag{15}$$

Combining with (10) yields

$$w'_{12} = w'_{\text{avg}} + \frac{e_{\text{RDI}}}{2\sqrt{2} \tan \beta} \tag{16}$$

$$w'_{34} = w'_{\text{avg}} - \frac{e_{\text{RDI}}}{2\sqrt{2} \tan \beta}, \tag{17}$$

where β is the transducer beam angle from the vertical as before. In order to derive beam-pair vertical velocities from earth-coordinate ADCP data,

1. earth coordinate vertical velocities are rotated into instrument coordinates ($w_{\text{avg}} \rightarrow w'_{\text{avg}}$),

2. expressions (16) and (17) are used to calculate w'_{12} and w'_{34}, and

3. the resulting beam-pair instrument velocities are rotated into a horizontal coordinate system.

The velocity transformations carried out by TRDI ADCPs are not as accurate as those derived with the algorithm described in Section C.1 for two reasons, both related to large tilt angles: i) Properly configured TRDI ADCPs use bin remapping at large tilt angles *(RD Instruments,* 1998). This nearest-neighbor interpolation scheme is less accurate than linear interpolation (e.g. *Ott,* 2002). ii) The instrument-to-earth transformation expression (13) is an approximation valid for small tilt angles *(Lohrmann et al.,* 1990). No evidence has been found so far suggesting that the inaccuracies associated with expression (13) are significant. Therefore, no attempt has been made to implement a correction.

---

[19]For upward-looking instruments, the first and third columns of the transformation matrix A1 are negated (first and second r.h.s. terms in expression (11)), which is equivalent to adding $180°$ to the roll angle *(RD Instruments,* 1998).

References

Deines, K. L., 1999: *Proceeding, CWTMC'99 (IEEE)*.

Firing, E. and R. Gordon, 1990: Deep ocean acoustic Doppler current profiling. *IEEE Fourth Working Conf. on Current Measurements*, 192–201.

Fischer, J. and M. Visbeck, 1993a: Deep velocity profiling with self-contained ADCPs. *J. Atm. Oc. Tech.* **10**, 764–773.

Fischer, J. and M. Visbeck, 1993b: Seasonal variation of the daily zooplankton migration in the Greenland Sea. *Deep Sea Res. I* **40**, 1547–1557.

Lohrmann, A., B. Hackett, and L. P. Røed, 1990: High resolution measurements of turbulence, velocity and stress using a pulse-to-pulse coherent sonar. *J. Atm. Oc. Tech.* **7**, 19–37.

Ott, M. W., 2002: An improvement in the calculation of adcp velocities. *J. Atm. Oc. Tech.* **19**, 1738–1741.

Polzin, K., E. Kunze, J. Hummon, and E. Firing, 2002: The finescale response of lowered ADCP velocity profiles. *J. Atm. Oc. Tech.* **19**, 205–224.

RD Instruments, 1998: ADCP coordinate transformation: Formulas and calculations. *RDI Manual*.

Thurnherr, A. M., 2010: A practical assessment of uncertainties in full-depth velocity profiles obtained with Teledyne/RDI Workhorse Acoustic Doppler Current Profilers. *J. Atm. Oc. Tech.* **27**, 1215–1227.

Thurnherr, A. M., 2011, March): Vertical velocity from LADCP data. *Proceeding, CWTMC'11 (IEEE)*.

Thurnherr, A. M., 2012: The finescale response of lowered ADCP velocity measurements processed with different methods. *J. Atm. Oc. Tech.* **29**, 597–600.

Thurnherr, A. M., S. S. Jacobs, P. Dutrieux, and C. F. Giulivi, 2014: Export and circulation of ice cavity water in Pine Island Bay, West Antarctica. *J. Geophys. Res.* **119**, 1754–1764.

Thurnherr, A. M., E. Kunze, J. M. Toole, L. St. Laurent, K. J. Richards, and A. Ruiz-Angulo, 2015: Vertical kinetic energy and turbulent dissipation in the ocean. *Geophys. Res. Lett.* **42**, 7639–7647.

Visbeck, M., 2002: Deep velocity profiling using Lowered Acoustic Doppler Current Profilers: Bottom track and inverse solutions. *J. Atm. Oc. Tech.* **19**, 794–807.